

Exploring group theory and topology for analyzing the structure of biological hierarchies

Shun Adachi*

Department of Microbiology, Kansai Medical University, 2-5-1 Shin-machi, Hirakata, Osaka 573-1010, JAPAN

Abstract

The concepts of population and species play a fundamental role in biology. The existence and precise definition of higher-order hierarchies, such as division into species, is open to debate among biologists. We seek to show a fractal structure of species by utilizing group theory, topology, and a set of zeta functions. First, we present a new metric, small s , that uses data from the natural environment to measure extents that are beyond the range of neutral (harmonic) logarithmic populations and are specific to a given species. We define this metric by modifying the Price equation, utilizing a Dirichlet series and an operator based on number theory. As expected, the box dimension of our model is $\dim_B A = 2$ and 2 is a critical line for the appearance of the fractal structure of species, which is confirmed by observation. Prime p numbers can be calculated from corresponding $\Im(s)$ values of non-trivial zero points of the Riemann zeta function. Integrating all methods, we are able to define a species as a p -Sylow subgroup of a particular community in a single niche, confirmed by topological analysis. Next, we show two ways of expression: a degenerate bosonic ψ function for describing fitness and a non-degenerate fermionic ϕ function for describing time development. We show that prime numbers may be related to speciation by considering discontinuities in the Riemann zeta function, including Bose-Einstein condensation, while prime closed geodesics of the Selberg zeta function may represent populations. Calculation of the norm of prime closed geodesics $|N(p)|$ shows that noninteracting adaptive species are in the mode $|N(p)| = 2/3$, while interacting neutral populations are in the mode $|N(p)| = 1$. The border between fluctuating populations and ordered species is $\Re(s) = 2$, as expected by various sets of fractal zeta functions. The mod 4 of primes corresponding to $\Im(s)$, the zero points of the Riemann zeta function and the Hurwitz zeta

function, reveal adaptive and disadaptive situations among individuals. Furthermore, our model has been partially successful at predicting transitions of biological phases. The time-dependent fitness function and the precise Hubble parameter of a fitness space can be predicted by the Schwarz equation. Finally, we introduce a Hodge-Kodaira decomposition for ϕ function to explain time development of the system. We thus posit a metric that is useful for discrimination between population data and species data. The significance of biological hierarchy is also discussed. In our patch with zeta dominance (PzDom) model, calculations only require knowledge of the density of individuals over time.

Keywords: Species, Community, Group theory, Topology, Riemann zeta function, Selberg zeta function

*Corresponding author.

E-mail address: f.peregrinusns@mbox.kyoto-inet.or.jp (S. Adachi)

1. Introduction

Living organisms encompass several levels of scaling and hierarchy. Inside cells, protein molecules are on the order of nanometers, and they cooperate or compete by activation or inhibition of specific biological activities. Normal eukaryotic cells are on the order of $10\ \mu\text{m}$, and their activities are the consequence of interactions between the molecules inside of them. In multicellular systems, each cell has its own role, and these combine to determine the interactions between the cells in the system. In nature, the number of individuals increases and decreases following the particular dynamics of that population, as characterized by their intrinsic physiology and the interactions between individuals. Molecular biology and ecology have already elucidated certain roles for the hierarchies that are inherent in living organisms. Therefore, to compare the dynamics of communities of various biological taxa, it is important to have a common definition of species. However, there are various ways to define species and none of them is commonly applicable to all the biological phenomena considered in the context of biology. First of all, we survey the history of the species concept, and then move on to what sort of definition we should consider to resolve all the entanglements of complex species phenomena, by utilizing mathematical ideas.

We start from population. Population, which is ranked just below species in the taxonomic hierarchy, is often defined both ecologically and demographically. [55] defines a population as “a group of organisms of the same species occupying a particular space at a particular time.” This is obviously a qualitative definition, and researchers utilize definitions of population that are appropriate in a given context. In contrast, the definition of a species has a long history of clarification. John Ray produced a biological definition of species in his *Historia Plantarum*: ... no surer criterion for determining species has occurred to me than the distinguishing features that perpetuate themselves in propagation from seed. Thus, no matter what variations occur in the individuals or the species, if they spring from the seed of one and the same plant, they are accidental variations and not such as to distinguish a species... Animals likewise that differ specifically preserve their distinct species permanently; one species never springs from the seed of another nor vice versa (translated by Silk, E.; [80]). Although he considered species as a static creation, it is important to note his foresight in distinguishing between variations within species and differences between species. In this paper, we further expand on this to form a definition based on discontinuities in the spectrum of the Selberg zeta function and the zero points of the Riemann zeta function. In his *Systema Naturæ*, Carl von Linné [103] presented systematic definitions of biological taxa in different hierarchies, such as species, genus, order, and class, and these were later followed by family, phylum, kingdom, and domain. He also established binomial nomenclature as a standardized way to write a scientific name. Although his idea of a species remained static, this enabled a systematic approach to a qualitative estimate of the relatedness among different living organisms. The static image of creationism itself was doubted following the *Philosophie Zoologique* of Jean-Baptiste de Lamarck [20], in which Lamarckian inheritance was proposed. Although this approach was ignored until recently, it has been reevaluated in recent studies of trans-generational epigenetic inheritance [10]. The idea of evolution was further developed as natural and sexual selection by Alfred Russel Wallace [107] in “On the tendency of varieties to depart indefinitely from the original type” and by Charles Darwin [17] in *On the Origin of Species*. However, the actual cause of speciation was still not understood. In his “Versuche über Pflanzenhybriden,” Gregor Mendel [65] proposed that genetic information might be important for plant hybridization and evolution; however, we now understand that the results of his experiments were achieved under hybridization of a plant species with different alleles, not actual hybrid species. The modern

definition of species is both an evolutionary and reproductive concept, and was described by Ernst Mayr in *Systematics and the Origin of Species* [63] as follows: “Species are groups of actually or potentially interbreeding natural populations, which are reproductively isolated from other such groups”. Until now, the essence of the difference between the concepts of population and species has been whether the concepts themselves are ecological/physical or evolutionary/genetic in nature. However, complex situations may arise in which a combined definition is required, and it may be difficult to determine whether the obtained data originated from populations or species, due to ambiguities in the overlapping definitions [15, 112]. For example, in “ring species”, there are continuous phenotypic characteristics and reproductive viability between physical neighbors, in contrast to reproductive inviability between the physical edges of the species. This means that reproductive isolation alone cannot be used to properly define a species. In contrast, reports of sympatric speciation demonstrate the metaphysical existence of species and speciation with discontinuity, even in environmentally nonisolated situations (e.g., [6]). It has been claimed that a biological species is a mere concept that describes unification of individuals and their genotypes within the population and populations within the species, by gene exchange resulting from bisexual reproduction and migration. Thus, the degree of this unification should be correlated with the presence of bisexual reproduction, although in reality, this correlation is very low, and uniparental species often differ very little from their biparental relatives living in similar conditions. Thus, isolated populations of biparental species often retain their specific identity for a long time, in spite of the absence of gene exchange and efficiency of migration [79]. We partially solved this, at least for Japanese *Dictyostelia*, by decoupling the short-term ecological time scale from the long-term evolutionary time scale, which differ on the order of 10^{17} [1]. That is, populations can be “neutral” within themselves, but an assemblage of populations as a whole is not always neutral. Therefore, the characteristic time scale of species/gene flow is assumed to be entirely different from that of population/migration.

However, the situations are complex and it is very likely that we need a simpler definition for pragmatic analyses of species. Let us start from simple philosophical logic. When we regard a certain level of hierarchy, the level has to possess identity. To maintain its identity requires adaptation to the environments in natural systems. The biological term ‘adaptation’ is thus integrated to a basic idea in evolvable systems with hierarchy. If we start from a certain level of the hierarchies where adaptation is obviously

applicable (such as the individual level, or in our case, metapopulation: a set of local populations that are linked by dispersal), by utilizing a proper morphism associated with the hierarchies, reoccurrence of a certain indicator value in an adaptive hierarchy among the sequence of the morphisms indicates there is another level of hierarchies with adaptation, proving the existence of the hierarchy. Therefore, if we select a proper set of indicator value and morphism, we can recognize the actual hierarchy in nature with adaptation.

Thus, we introduce group theory to our model as an example of such a morphism. A set G can be regarded as a group if G is accompanied by an operation (group law) that combines any two elements of G and satisfies the following axioms. (i) closure: a result of an operation is also an element in G ; (ii) associativity: for all a_G, b_G and c_G in G , $(a_G b_G) c_G = a_G (b_G c_G)$; (iii) identity element: for all elements a_G in G , there exists an element 1_G in G such that $1_G a_G = a_G 1_G = a_G$ holds; (iv) inverse element: for all a_G in G , there exists an element a_G^{-1} such that $a_G a_G^{-1} = a_G^{-1} a_G = 1_G$. Next, we move forward to the nilpotent group. If a group G has a lower central series terminating in the trivial subgroup after finitely many steps: $G = G_0 \supset G_1 \supset \dots \supset G_j = \{1_G\}$ where at all $i = 1, 2, \dots, j$, $G_{i-1}/G_i \subset [\text{a center of } G/G_i]$. If a group is a nilpotent group, after finitely many steps (or, in other words, finitely many time steps), it can converge to a certain identity. In this regard, let us consider a nilpotent group G represents a status identity of a certain community in a particular niche.

We next investigate ‘‘Sylow theorems’’ [95] as relevant to our context. The necessary and sufficient condition for a finite group G being a nilpotent group is that an order n of G can be prime factorized as $p_1^{l_1} p_2^{l_2} \dots p_g^{l_g}$ and for each $i = 1, 2, \dots, g$, every subgroup N_i (as p_i -Sylow subgroup) is a normal subgroup in G . When the left coset $a_G H$ is equivalent to the right coset $H a_G$ of subgroup H in G with an element a_G , H is a normal subgroup of G . N_i satisfies a subgroup in G with an order of $p_i^{l_i}$ and it is a p_i -Sylow subgroup. It is also true that the number of subgroups with an order $p_i^{l_i}$ in G is (a multiplication of) $p_i + 1$ and all of them are conjugate. Conjugate of H means $a_G H a_G^{-1}$ with a_G in G . In this sense, p_i can label a subgroup of community (from now on, provisionally regarded as ‘‘species’’). l_i is a particular dimension of the species. Normality of N_i is trivial when the group is abelian. Conjugacy means that genetics within a species is mathematically in equivalence relation. Therefore, if we can adopt a robust method for calculating p_i, l_i values with an operation of group (here, simply multiplication is enough), we can mathematically regard a species p_i as a subgroup of a

community G . Later, we will demonstrate the exact calculation procedure concomitantly with characterization of the model with empirical data on the Dictyostelia community in Izu of Japan, to show the applicability of the model to actual biological hierarchies, especially with population, species, and community dynamics.

We would like to further clarify a metric that can be used to discriminate between the dynamics of populations/species, based on fractals, as an example of an indicator value described earlier. We will use the following definitions in our analysis, which is based on empirical data obtained from a natural environment. We define a population as *a group of individuals of a species inhabiting the same area and time*, and a **species** as ***a sum of populations with genetically close relationships distinguishable by discontinuity of genetic distances among different species specific to each niche, characterized by a p -Sylow subgroup***. In this sense, “ring species” is a single species, not constituted by different species.

In this way, a species cannot be disentangled from the actual interactions that constitute a community, with certain sorts of entanglements among species. The history of social interactions in biology began with William Donald Hamilton’s “The genetical evolution of social behavior I” [33], “The genetical evolution of social behavior II” [34], John Maynard Smith’s “Group selection and kin selection” [89], and George Robert Price’s “Selection and covariance” [77]. They established that genetic relatedness is important for maintaining cooperative phenotypes and evolution of living organisms. For co-evolvable nonrelatives, it is important to consider how reciprocal altruism maintains cooperation, as proposed in Robert Trivers’s “The evolution of reciprocal altruism” [101]. Finally, multilevel selection theories have been proposed, such as those presented in “Reintroducing group selection to the human behavioral sciences” [114] and *Unto Others: The Evolution and Psychology of Unselfish Behavior* [90]. These theories can explain the actual cooperative selection process of individual genes that are distantly related within a cell or an individual as a reproduction unit. Although there is a claim to group selection based on elementary mathematics (refer [90]), the modern approach from mathematics shows that this is theoretically untenable because it neglects set-theory. This elementary approach also assumes significantly long durations of environmental constancies, which is not likely to always hold in actual empirical contexts. Biological hierarchies are thus regarded as an important idea for analysis of an evolutionally process. Despite the lack of agreement among biologists, information theory can be used

to analyze the dynamics of the concomitantly observed scales. However, the extent of genetically close relationships between different species cannot easily be distinguished from that of populations in a genetic sense. Therefore, we present a new metric for defining a species, especially for use in adaptive situations: we found that the norm of geodesic successfully discriminates between adaptive species ($|N(p)| = 2/3$) and chaotic population/species ($|N(p)| = 1$). To evaluate the metric, we need a model system. A candidate model is that presented by Kimura (1964) in the theory of diffusion equations in population genetics. In the model, genetic characteristics are used to demonstrate the dynamics. Unlike the original genetic model, here, instead of gene frequencies, we investigate dynamics using the ratio of the number of individuals to the whole population. This means combining genetic information and environmental effects with the number of individuals. We note that spatially distributed models that assume knowledge of underlying stochastic processes, which are usually drawn from birth/death, immigration/emigration, mutation/speciation, and niche differentiation, were developed to further understand the nature of observed populations and species (e.g., [58]). In the unified neutral theory [38, 39, 14], a local community (an ecological unit composed of a group of organisms or a population of different species occupying a particular area, usually interacting with each other and their environment) dominates a population of a few species and results in extinction of rarer species, deviates from the neutral logarithmic distribution observed in dominant species and rare species. A metacommunity is a set of local communities that are linked by dispersal, and on this scale, there is greater biological diversity; a nearly logarithmic distribution is observed for the population abundance of ranked species. As with the diffusion equation model from population genetics, the distribution depends not on individual adaptations but on random ecological drift that follows a Markov process [38, 39]; that is, information entropy, as measured by the Shannon index, is maximized [86, 36, 5]. Idiosyncrasies seem to be involved in Hubbell's theory ([78]; see also [1]). There is also a report that considers the Max-Ent (a model for a force that maximizes entropy during time development) of geographic distribution [72]. Thus, the unified neutral theory is part of information theory. It has three characteristic parameters: population size, point mutation rate, and immigration rate. Note that we only utilize the $N_k/\Sigma N = \phi = C\bar{w}^N$ (a normalized fitness) part of Kimura's theory without including the Hardy-Weinberg principle. Our model is unrelated to gene frequencies of different alleles as in the Hardy-Weinberg principle, because we

utilize $C\bar{w}^N$, not $C\bar{w}^N x^{2N\nu-1}(1-x)^{2N\mu-1}$ with gene frequency x . Therefore, in our model, it is not necessary to assume genetic equilibrium. Also note that we only utilize Hubbell’s theory as a basis for calculating the extent of the difference from an ecologically neutral situation. By modifying these theories, we are able to distinguish neutral populations with a shorter time scale from adaptive species with a longer time scale for a set of observed data of Dictyostelia; this data set had a significantly small immigration rate ($m_i < 10^{-3}$) [1]. We also consider effects due to the randomness of population dynamics and the directionality of species dynamics in nature together; this is in addition to the theoretical randomness discussed by [29] and the theoretical directionality (i.e., Bose-Einstein condensation) discussed in [7].

We propose an original model that uses a different definition of entropy (relative entropy) than that used by [36] and a new definition of temperature: an integrative environmental parameter that determines the distribution of population/species deduced from the logarithmic distribution of populations/species. The units of this parameter are set to cells/g, and it is a half-intensive parameter, as described in the first parts of Results. We define new metrics that are based on statistical mechanics [30, 5, 97] to distinguish and interpret species and population counts in mixed communities; we apply this to an actual community of Eastern Japanese Dictyostelia [1]. The use of statistical mechanics to interpret biological systems began with [60], proceeding to the disastrous complexity of the Hamiltonian described by [44], and continued with the Lotka-Volterra equations of N-interacting species in an artificially noisy environment [91]. [44] also posited an interesting model for a time-developing system; however, Kerner’s model and our model belong to different mathematical spaces, and a set of mathematically rigorous studies is required to precisely describe their interrelationships. This is different from a time-dependent ecosystem assembly model that is restricted to finite Markov chains, such as was proposed by [73] or [13]. We will describe the nonrandom directionality of the model, which is based on number theory with $|N(p)| = 2/3$. Importantly, we are able to calculate the different sets of critical temperatures and Weiss fields (with Bose-Einstein condensation) at which various natural first-order phase transitions take place among species or populations (where by ‘phase transitions’ we mean a community moves from chaos caused by neutrality or nonadaptive situations and results in an increase of or domination by a particular species, or moves from that to domination by a particular population within a species). The order parameter in this model is large S . This complex phase transition nature of different hier-

archies in the wild was not fully explained by [36]; it was briefly mentioned by [5] as part of the relative entropy. The model shows that the populations of some highly adapted species are much more stable than those of others.

To the best of our knowledge, no previous studies have considered the biological view proposed herein. We introduce an index, small s , to distinguish between populations and species; the value of the real part of this index is high for an ordered species and low for a fluctuating population in the wild; that is, $\Re(s) = 2$ is a critical line for both, in strong agreement with fractal theory of a box dimension $\dim_B A = 2$ with a model \mathbb{R}^2 , which is the case for our s metric. To begin, we modified the Price equation [77] to develop our index, small s , which is based on the $R = T$ theorem and Weil's explicit formula [109, 98, 113]. The Price equation describes evolution and natural selection, and here it is used to replace gene frequencies with the proportion of individuals in a given population or species. The small s index is related via covariance and expectation to the Price equation. The nontrivial zeros of the Riemann ζ function provide information about the bursts or collapses of a population. In this model, speciation is thus related to prime numbers; that is, a prime ideal indicates the status of a specific species in the system, and time-dependent multiplication of the fitness can be calculated by utilizing these primes. We then calculate the unique equations of the model in the Maass form and examine the spectra of the data. Use of the Selberg zeta and Hasse-Weil L to calculate the norm of prime closed geodesics $|N(p)|$ clarifies that the noninteracting adaptive species world (an integrative space of time and other dimensions) is in the mode $|N(p)| = 2/3$, while the interacting neutral populations are in the mode $|N(p)| = 1$. Combining these calculations with phylogenetical asymmetry, we determine whether the observed hierarchy of data represents chaotic populations/nonadaptive species or adaptive species in genuinely successful niches. Our model has been partially successful at predicting imminent transitions between biological phases (adaptation/disadaptation). By utilizing the Schwarz equation, we also determined the time-dependent fitness function that matches the observations. Additionally, web-based formalism [32] based on a combination of supersymmetry (Hodge-Kodaira decomposition of a non-degenerate fermionic ϕ function) and an analogy to the transactional interpretation of quantum mechanics leads to a nine-dimensional model without time (three-dimensional nature \times three-dimensional fluctuations). The idea of a fitness space leads to a precise time-dependent Hubble parameter for that space, for an appropriate timescale. Finally, the nature of asymmetric time devel-

opment of ϕ within our model is elucidated, and a degenerate ψ (fitness) function also deduces some aspects of future. Recently Rodríguez and colleagues reported a physical framework for applying quantum principles to ecology (e.g., [82, 84]); however, this was based on thermodynamics, or on physical principles, not biological information, and is different from the more mathematical/informational, nonthermodynamical approach described here. The proposed model combines information theory and observations from nature to bring new understanding to the biological ideas of population and species; this is different from the physical and theoretical thermodynamical approach used by [102]. Here, a patch is defined to be a small plot or piece of land, especially one that produces or is used for growing specific organisms. We call our model the patch with zeta dominance (PzDom) model, and it is only necessary to evaluate $\Re(s)$ to determine whether a population is chaotic or dominated by species; the border is at $\Re(s) = 2$. The model requires only the change in density of individuals over time. We will also discuss the significance of biological hierarchies. We propose an approach that will allow future research to explore the nature of hierarchical systems.

2. Materials and Methods

The data for the number of individuals in each population and species were obtained from natural (nonlaboratory) environments. The sampling method is described in [1]. Field experiments were approved by the Ministry of the Environment (Japan), Ministry of Agriculture, Forestry and Fisheries (Japan), Shizuoka Prefecture (Japan) and Washidu Shrine (Japan). The approval Nos. are 23Ikan24, 24Ikan72-32, and 24Ikan72-57.

Soil samples were obtained from two point quadrats of the Washidu region of Izu in Japan. The number of individual cellular slime molds per gram of soil was determined by counting the number of plaques cultivated from soil samples. Species were identified by both morphology and by the DNA sequences of the 18S rRNA genes. Samples were obtained in each month from May 2012 to January 2013 inclusive. Calculations were performed using Microsoft Excel 12.3.6, wxMaxima 15.04.0, R 3.3.2 and GNU Octave 3.8.0.

In more detail, sampling occurred at two 100 m² quadrats in Washidu (35°3'33"N, 138°53'46"E; 35°3'45"N, 138°53'32"E). Within each 100 m² quadrat, nine sample points were established at 5 m intervals. From each sampling point, 25 g of soil was collected. Cellular slime molds were isolated from

these samples as follows. First, one sample from each site was added to 25 ml of sterile water, resuspended, and then filtrated with sterile gauze. Next, 100 μ l of each sample solution was mixed with 100 μ l of HL5 culture medium containing *Klebsiella aerogenes* and spread on KK2 agar. After two days of storage in an incubator at 22 °C, the number of plaques on each agar plate was recorded. Note that the number of plaques corresponds to the total number of living cells at any possible stage of the life cycle. That is, the niche considered here is the set of propagable individuals of Dictyostelia; these are not arranged in any hierarchy or by stage in the life cycle. Also, note that we did not examine the age or size structure of organisms, since most of these were unicellular microbes. Mature fruiting bodies, consisting of the cells from a single species, were collected along with information regarding the numbers of plaques in the regions in which each fruiting body was found. Finally, spores were used to inoculate either KK2 for purification or SM/5 for expansion. All analyses were performed within two weeks from the time of collection. The isolated species were identified based on 18S rRNA (SSU) sequences, which were amplified and sequenced using PCR/sequencing primers, as described in [64] and the SILVA database (<http://www.arb-silva.de/>). The recipes for the media are described at <http://dictybase.org/techniques/media/media.html>.

3. Results

3.1. Universal equation for population/species dynamics based on the Price equation and logarithms

The neutral logarithmic distribution of ranked biological populations, for example, a Dictyostelia metacommunity [1], can be expressed as follows:

$$N_k = a - b \ln k, \quad (1)$$

where N is the population density or the averaged population density of species over patches, and k is the index (rank) of the population. The parameters $a \approx N_1$ and the rate of decrease b are derived from the data by sorting the populations by number rank. We also applied this approximation to an adaptive species to evaluate the extent of their differences from neutral populations [1]. We note that this approximation is only applicable to communities that can be regarded as existing in the same niche, and not to co-evolving communities in nonoverlapping niches.

Based on the theory of diffusion equations with Markov processes, as used in population genetics [45], we assume that the relative abundance of the

populations/species is related to the N th power of D ($= \bar{w}$ in [45]) multiplied by the relative patch quality P ($= C$ in [45]) (that is, $PD^{N_k} = C\bar{w}^{N_k} = \phi = N_k/\Sigma N$; see also [45]). In this context, D^{N_k} represents the relative fitness of an individual; this varies over time and depends on the particular genetic/environmental background and the interactions between individuals. P is a relative environmental variable and depends on the background of the occupying species; it may differ within a given environment if there is a different dominant species.

To better understand the principles deduced from Kimura's theory, we introduce the Price equation [77]:

$$w_k \Delta z = \text{Cov}(w_k, z_k) + E(w_k \Delta z_k). \quad (2)$$

Remember $N_1 = kN_k$ when the distribution is completely harmonic (neutral). Note that $z = \ln(k \cdot N_k)/\ln k = 1 + \ln N_k/\ln k$, where $k \neq 1$ and $z = +\infty$ when $k = 1$; we use this instead of gene frequency in Price's original paper. The relative distance between the logarithms of norms N and the rank k will be discussed below when we consider the Selberg zeta analysis [40]; here, $\ln k$ is the relative entropy from a uniform distribution as a (in other words, it is a Kullback-Leibler divergence $D_1(P||Q) = \sum_{i=1}^n p_i \ln \frac{p_i}{q_i}$ of $n = 1, p_i = 1, q_i = 1/k$, the interaction probability from the first ranked population/species; thus we are able to calculate the deviation from a logarithmic distribution, and both logarithms are topological entropies). Next, we assume that for a particular patch, the expectation of the individual populations/species is the averaged (expected) maximum fitness; this is D to the power $E(\Sigma N)$ th, when $E(\Sigma N)$ is the average N among all populations or the sum of the average N over all patches among all species ($|D_k|^{E(\Sigma N)}$). This is a virtual assumption for a worldline (the path of an object in a particular space) because a population seems to be in equilibrium when it follows a logarithmic distribution [38, 39, 1] and species dominate [1]. We will prove below that the scale-invariant parameter small s indicates adaptations in species in neutral populations. Under the assumptions in this paragraph, $E[w]$ is $|D_k|^{E(\Sigma N)}$ and $E[z]$ is approximately $\ln N_1/\ln k$. If we set $w = |D_k|^{E(\Sigma N)} - \Delta z$, $N_k = D^{N_k}$ and $k \neq 1$, $\Delta z \approx \Delta N_k \ln D_k/\ln k$ with $D_k \sim 1$. When $k = 1$, $\Delta z = \infty$ but Δz is removed from the calculation by an identical Δz anyway, upon introduction of the equation below. Dividing the Price equation by Δz , we obtain

$$w_k = \frac{\ln \frac{N_1}{N_k}}{\ln k} - 1 + |D_k|^{E(\Sigma N)} (k \neq 1). \quad (3)$$

Recall $N_1 = kN_k$ when the distribution is harmonic (normal). In this case, $\ln \frac{N_1}{N_k} = \ln k$ and $\frac{\ln \frac{N_1}{N_k}}{\ln k}$ becomes 1. The value of this calculation represents the deviation from the harmonic (neutral) distribution. We will consider the case when $k = 1$ in a later subsection; see Eqns. (22) and (23). For simplicity, we denote $1 + \text{Cov}/\Delta z : \frac{\ln \frac{N_1}{N_k}}{\ln k}$ as $\mathfrak{R}(s)$ and $E(w_k) : |D_k|^{E(\Sigma N)}$ as $\mathfrak{S}(s)$. Now think of a Dirichlet series $\sum_{j=1}^{\infty} b_{Dj} l_{Dj}^s$. An upper limit of box dimension of this system A (a subset of \mathbb{R}^2) is:

$$\overline{\dim}_B A = \limsup_{n \rightarrow \infty} \frac{1}{\ln l_{Dn}^{-1}} \ln \left(\sum_{j=1}^n b_{Dj} \right) \quad (4)$$

[12]. If we regard $\lim_{n \rightarrow \infty} \sum_{j=1}^n b_{Dj} = \frac{N_1}{N_k}$ and $\lim_{n \rightarrow \infty} l_{Dn} = \frac{1}{k}$, such a Dirichlet series fulfilling this condition is characteristic of the model we are considering; dimensions large enough can achieve such approximations close to lim. When $s = 1$, the Dirichlet series will be a set of: $\frac{N_1}{kN_k}$, the deviation from logarithmic distribution of N , setting a datum point as 1.

Now we know $\mathfrak{R}(s)$ is an upper limit of fractal dimension of A , characterized by the Dirichlet series. Next, consider a distance zeta function for \mathbb{R}^2 :

$$\zeta_A(s) := \int_{A_\delta} d(x, A)^{s-N} dx, \quad (5)$$

when A_δ is a δ -neighborhood of A , $d(x, A)$ is a distance from x to A and $N = 2$. As there is a critical line $\{\mathfrak{R}(s) = \overline{\dim}_B A\}$ and $\zeta_A(s)$ is only defined in $\mathfrak{R}(s) > N$ when $|\bar{A}| > 0$ ($\dim_B A = N$) [57], $\mathfrak{R}(s) = 2$ is the critical line for our fractal model and it is confirmed by observation in later sections. From this theory, fractal structure from population to species can only appear beyond $\mathfrak{R}(s) = 2$ in our \mathbb{R}^2 model and it is statistically confirmed later on.

To explain this more carefully, consider a tube zeta function [57]:

$$\tilde{\zeta}_A(s) := \int_0^\delta t_t^{s-N-1} |A_t| dt_t. \quad (6)$$

This is a w analogue of s distance zeta function. Whether A is Minkowski nondegenerate or degenerate is tested by analyzing $\dim_B A$ -dimensional Minkowski contents $\mathcal{M}^{\dim_B A}(A)$ ($*$ or $*$ notes lower or upper limit). If $0 < \mathcal{M}_*^{\dim_B A}(A) \leq \mathcal{M}^{*\dim_B A}(A) < +\infty$, it is Minkowski nondegenerate. If $\mathcal{M}_*^{\dim_B A}(A) = 0$ or $\mathcal{M}^{*\dim_B A}(A) = +\infty$, it is Minkowski degenerate. Since $|A_t| = t_t^{N-\dim_B A} (F(t_t) +$

$o(1)$) as $t_t \rightarrow 0^+$, $\liminf_{t_t \rightarrow 0^+} F(t_t) = \mathcal{M}_*^{\dim_B A}(A) = 0$ in the equation above if the tube zeta function is definable. Therefore, A is Minkowski degenerate in the sense of w . Furthermore, consider a tube zeta function (for second kind, newly defined here with s) as:

$$\tilde{\zeta}_{2A}(s) := \int_0^\delta t_t^{s-N} |A_t| dt_t. \quad (7)$$

If we set $t_t = d(x, A)$, $\tilde{\zeta}_{2A}(s) \approx \int_0^\delta F(t_t) dt_t$. If the zeta function converges to but does not equal 0, it should neither be $\mathcal{M}_*^{\dim_B A}(A) = 0$ nor $\mathcal{M}^{*\dim_B A}(A) = +\infty$ ($\limsup_{t_t \rightarrow 0^+} F(t_t) = \mathcal{M}^{*\dim_B A}(A) = +\infty$). Thus A is Minkowski nondegenerate in the sense of s .

Note that $w = s - 1$, and w and s correspond to the R -charges of the bosonic ψ and fermionic ϕ functions, respectively. Note also that w may be stacked as a boson with other individuals in the fitness space, s is derived from w , and the s value is a mutually exclusive existence related with time development as shown later together with supersymmetry.

Next, we move on to $\{0 < \Re(s) < N\}$ (please also refer to [57]). For this criterion, think of relative fractal drum (A, Ω) :

$$A_{\mathcal{L}} = \{a_{k_a} = \sum_{j=k_a}^{\infty} \ell_j : k_a \in \mathbb{N}\}, \Omega_{\mathcal{L}} = \bigcup_{k_a=1}^{\infty} (a_{k_a+1}, a_{k_a}) \quad (8)$$

where $\mathcal{L} = (\ell_j)_{j \geq 1}$ and $(\ell_j)_{j=1}^{\infty}$ is an infinite nonincreasing sequence of positive numbers such that $\sum_{j=1}^{\infty} \ell_j < \infty$. We can set $a_{k_a} = |\zeta(\Re(s))|$ when $\Re(s) > 0$ and $\Re(s) \neq 1$. In $\Re(s) = 1$, we can set $a_{k_a} = \frac{E(\sum N)}{N_1}$ as in the next section. Set a relative tube zeta function:

$$\tilde{\zeta}_{A,\Omega}(s) := \int_0^\delta t_t^{s-N-1} |A_t \cap \Omega| dt_t. \quad (9)$$

And also, a window:

$$\mathbf{W}_w = \{s \in \mathbb{C} : \Re(s) \geq S(\Im(s))\} \quad (10)$$

where the function screen $S : \mathbb{R} \rightarrow (-\infty, D(\zeta_A)]$ and an abscissa $D(\zeta_A) := \inf\{\alpha \in \mathbb{R} : \int_{A_\delta} d(x, A)^{\alpha-N} dx < \infty\}$. Additionally, $\mathcal{P}(\zeta_A, \mathbf{W}_w) = \{\omega \in \mathbf{W}_w : \omega \text{ is a pole of } \zeta_A\}$.

A distributional fractal tube formula of level $k_l = 0$ is:

$$|A_t \cap \Omega| = \sum_{\omega \in \mathcal{P}(\tilde{\zeta}_{A,\Omega}, \mathbf{W}_w)} \text{res}(t_t^{N-s} \tilde{\zeta}_{A,\Omega}(s), \omega) + \tilde{\mathcal{R}}_{A,\Omega}^{[0]}(t_t), \quad (11)$$

where

$$\langle \tilde{\mathcal{R}}_{A,\Omega}^{[k_l]}, \varphi \rangle = \frac{1}{2\pi i} \int_S \frac{\{\mathfrak{M}\varphi\}(N-s+1+k_l)}{(N-s+1)_{k_l}} \tilde{\zeta}_{A,\Omega}(s) ds, \quad (12)$$

$\{\mathfrak{M}f\}(s) := \int_0^{+\infty} t_t^{s-1} f(t_t) dt_t$ and $\varphi \in \mathcal{H}(0, \delta)$ ($\mathcal{D}(0, \delta) := C_c^\infty(0, \delta)$, $C_c^\infty(0, \delta)$ is a space of infinitely differentiable complex-valued test functions with compact support contained in $(0, \delta)$ and $\mathcal{D}(0, \delta) \subseteq \mathcal{H}(0, \delta)$). $\tilde{\mathcal{R}}_{A,\Omega}^{[0]}(t_t)$ will give you the residual of $|A_t \cap \Omega|$.

Now we consider a relative shell zeta function:

$$\check{\zeta}_{A,\Omega}(s; \delta) := - \int_0^\delta t_t^{s-N-1} |A_{t,\delta} \cap \Omega| dt_t \quad (13)$$

where $A_{t,\delta} := A_\delta \setminus A_t^c$. If (A, Ω) is a Minkowski nondegenerate,

$$\mathcal{M}_*^{\dim_B A}(A, \Omega) \leq \text{res}(\check{\zeta}_{A,\Omega}, \dim_B A) \leq \mathcal{M}^{*\dim_B A}(A, \Omega). \quad (14)$$

That is, except the case for $\Re(s) = 1$ with an observer of the system, this condition is fulfilled in the sense of s . However, it is not Minkowski measurable because $|A_t \cap \Omega|$ is not approaching 0 and thus $\lim_{t_t \rightarrow 0^+} t_t^{-N-\dim_B A} |A_t \cap \Omega|$ does not converge [57]. In the sense of w , (A, Ω) is a Minkowski degenerate. For $\Re(s) = 1$, there is a possibility $\check{\zeta}_{A,\Omega}$ converges and assuming the observer exists, it does converge despite not being Minkowski measurable. Therefore in all the situations there is chaos observed from $\Re(s) = 1$, predicted by $\tilde{\mathcal{R}}_{A,\Omega}^{[0]}(t_t)$. $\Re(s) = 2$ is mathematically cumbersome to characterize and similar analyses for it are beyond the scope of this paper [57].

3.2. Introducing $\Re(s)$ allows us to distinguish types of neutrality

Zipf's law is used to statistically analyze probability distributions that follow a discrete power law. For example, if the distribution of N can be approximated by a logarithmic relation with parameter k , then Eqn. (1) holds. Zipf's law is related to the Riemann zeta function $\zeta(s) = \sum_{n=1}^{\infty} \frac{1}{n^s}$ as follows:

$$|P_k||D|^{N_k} = f_s(k) = \frac{1}{k^{\Re(s)}|\zeta(s)|} = \frac{N_k}{E(\Sigma N)}, \quad (15)$$

and this will normalize the k th abundance by $E(\Sigma N)$. We set absolute values of $|\zeta|$ and $|P_k|$ for approximating both the $s > 1$ ($\zeta > 0$, $N_k < N_1/k$) and $s < 1$ ($\zeta < 0$, $N_k > N_1/k$) cases. If we set the density matrix to be $\rho_d = \frac{N_k}{E(\Sigma N)}$, then the von Neumann entropy would be $S_{vN} = -\text{tr}(\rho_d \ln \rho_d)$. Note that this model is a view from the first-ranked population, and either cooperation or competition is described by the dynamics/dominancy of the population. The partial trace of state $A(k = 1)$ over $B(k \neq 1)$ is $\rho_A = \text{tr}_B \rho_{AB}$. To examine the difference between population and species dynamics, linearization of the above model leads to

$$\frac{\Delta N_k}{E(\Sigma N)} = -\frac{\Delta \zeta}{k^{\Re(s)} |\zeta|^2}. \quad (16)$$

Therefore, $\Delta N_k > 0$ implies $\Delta \zeta < 0$, $\Delta N_k < 0$ implies $\Delta \zeta > 0$, and $\Delta N_k = 0$ implies $\Delta \zeta = 0$. Each of the local extrema of ζ thus represents a pole for the population/species, and a large (resp. small) value of $|\zeta|$ represents a small (resp. large) fluctuation. Only those points of ζ that are close to zero represent growth bursts or collapses of the population/species. According to the Riemann hypothesis, at these points, the following equation will approximately hold for the fitness w : $[\Re(s-1) = 1/2]$ and $[\Re(s-1) = -2l_s, \Im(s) = 0]$ (negative values for s will be characterized later), where l_s is a natural number independent of the population/species rank.

Taking the logarithm of Eqn. (15), we obtain

$$N_k = \frac{1}{\ln D_k} \ln \frac{1}{P_k \zeta(s)} - \frac{s}{\ln D_k} \ln k, \quad (17)$$

$$-\ln D_k \cdot N_k = \ln P_k \zeta(s) + s \ln k. \quad (18)$$

Therefore,

$$a = \frac{-\ln P_k \zeta(s)}{\ln D_k}, \quad (19)$$

$$b = \frac{s}{\ln D_k}, \quad (20)$$

$$\Re(s) = \frac{\ln \frac{N_1}{N_k}}{\ln k} (k \neq 1), \quad (21)$$

$$\zeta(s) = \frac{E(\Sigma N)}{N_1} \geq 1 (k = 1 \text{ in species}), \quad (22)$$

$$\Re(s) = 1 (k = 1 \text{ in population/observer}), \quad (23)$$

$$D_k = e^{\frac{s}{b}}, \quad (24)$$

$$P_k = \frac{1}{D_k^a \zeta(s)}. \quad (25)$$

$\Re(s)$ is obviously scale invariant if k is a fixed number in a particular system. Note that s and $\zeta(s)$ can thus be approximated using data from the distribution of N . When $k = 1$ for a given population, s can be defined as 1 because the distribution is almost harmonic. When $k = 1$ for a given species, s can be better calculated by an inverse function of ζ , because in this situation the distribution is no longer harmonic. For convergence, it is necessary that $N \sim 0$, $s \sim 1$, $\zeta \sim \pm\infty$, and $P \sim 0$. We will also assume that $s = +\infty$ and $\zeta = 1$ when a single population/species is observed. In [1], we analyzed s values using both the relative abundances of the population and the species; we determined that they give significantly different results (see Figure 1 and Table 1). The population values are restricted to between 0 and 2, while those of the species are often greater than 2. This proves that populations behave neutrally below $\dim_B A = 2$, while species are more likely to dominate above $\dim_B A = 2$; this will be discussed in more detail below. When s is larger than 2, the dynamics correspond to that of species, as will be discussed below. In Table 1, 6/54 s values greater than 2 are highlighted in red; this indicates that these were not observed in a population of 162 samples ($p \sim 4 \times 10^{-45}$ for χ^2 -test). In the following, the parameter s is the small s of this model. Note that when $k \neq 1$, the calculation of $\Re(s)$ is the same for both a population and a species, and the border $\Re(s) = 2$ clarifies the distinction of a neutral population ($0 < \Re(s) < 2$) versus a dominant species ($\Re(s) > 2$) as expected in the fractal theory described earlier.

If $D_k \sim 1$, there are two possibilities: (i) $P_k \approx 1/\zeta(s) \approx \Sigma\mu(n)/n^s$ (where μ is the Möbius function) must be true for a to converge, and for b to converge, we need $s \sim 0$; (ii) For N to converge, we need $s \sim 1$ when $P_k \ll 1$. In this case, we have $kP_k \approx 1/\zeta(s)$. When (i) holds, we have true neutrality among the patches. Both (i) and (ii) can be simply explained by a Markov process for a zero-sum population, as described in Hubbell (2001). In both cases, $f_s(k) \sim P_k$, and the populations are apparently neutral for D . When there is true neutrality in both the populations and the environment, $P_k \approx 1/\zeta(s) \approx \Sigma\mu(n)/n^s$, we say that there is *Möbius neutrality*. When there is apparent neutrality of D with $s \sim 1$, we say that there is *harmonic neutrality*. The value of s can thus represent the characteristic status of a

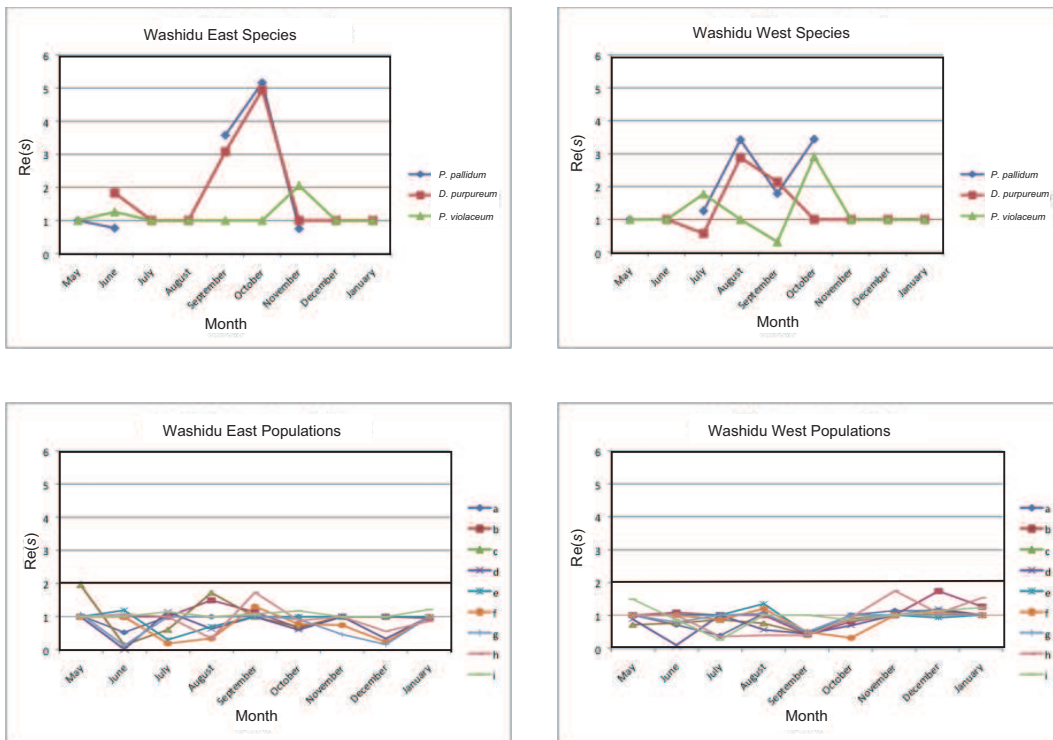


Figure 1: Dynamics of $\Re(s)$ over time for species and populations in two quadrats. *P. pallidum*: *Polysphondylium pallidum*; *D. purpureum*: *Dictyostelium purpureum*; *P. violaceum*: *Polysphondylium violaceum*. The top two panels present data for three different species, and the lower two panels present data for nine different point quadrats.

Table 1: $\Re(s)$ and N values.

$\Re(s)$	<i>P. pallidum</i> (WE)	<i>D. purpureum</i> (WE)	<i>P. violaceum</i> (WE)	<i>P. pallidum</i> (WW)	<i>D. purpureum</i> (WW)	<i>P. violaceum</i> (WW)			
May	-	-	-	-	-	-			
June	0.7693	1.8305	1.258	1.2619	0.5752	1.7742			
July	-	-	-	3.4223	2.8795	-			
August	-	-	-	1.7897	2.1411	0.3186			
September	3.5762	3.0777	-	3.4417	-	2.3037			
October	3.1638	3.0423	-	-	-	-			
November	0.7481	-	2.056	-	-	-			
December	-	-	-	-	-	-			
January	-	-	-	-	-	-			
N	<i>P. pallidum</i> (WE)	<i>D. purpureum</i> (WE)	<i>P. violaceum</i> (WE)	<i>P. pallidum</i> (WW)	<i>D. purpureum</i> (WW)	<i>P. violaceum</i> (WW)			
May	0	76	0	0	83	0			
June	78	209	52	137	0	0			
July	1282	0	0	80	215	320			
August	1561	0	0	1330	181	0			
September	901	107	0	809	77	549			
October	1039	38	0	739	0	147			
November	60	0	101	336	0	0			
December	180	0	0	71	0	0			
January	29	0	0	99	0	0			
$\Re(s)$ WE	a	b	c	d	e	f	g	h	i
May	1.0336	1	1.9442	1	1	1	1.0821	1	1
June	0.5328	1	0.1545	0.0332	1.1928	1	0.1374	1.076	1.0071
July	1	1	0.6131	1.1497	0.3117	0.2016	1	1	1.148
August	1	1.4925	1.7167	0.6348	0.7075	0.3523	1	0.3502	1
September	1	1.1361	1	1	1	1.3035	1.0325	1.7248	1.085
October	1	0.6746	0.6937	0.6092	1	0.7836	0.9259	0.886	1.1746
November	1	1	1	1	1	0.7481	0.472	1	1
December	1	1	1	0.3429	1	0.2455	0.1712	0.5637	1
January	1	0.9516	1	1	1	1	1	0.8666	1.215
$\Re(s)$ WW	a	b	c	d	e	f	g	h	i
May	1	1	0.7125	0.8782	1	1	1	1	1.473
June	0.708	1.0735	0.7613	0.1056	1	1	0.7883	1	0.8612
July	0.3888	1	0.8635	1	1	0.8614	1	0.3629	0.263
August	1.0524	1	0.756	0.5644	1.3367	1.1911	1.0473	0.3985	1
September	0.4918	0.4236	0.4243	0.4427	0.4535	0.4969	0.5051	0.3985	1
October	1	0.8073	0.8982	0.6913	1	0.3219	1	0.9284	0.8523
November	1.1334	1	1	1	1	1	1	1.7235	1
December	1.1214	1.7164	1	1.1833	0.9208	1.0718	1	1.0594	1.1375
January	1	1.2501	1	1	1	1	1	1.5151	1.2228
N WE	a	b	c	d	e	f	g	h	i
May	680	0	94	0	0	1392	424	0	0
June	1120	0	2131	2580	221	2640	2270	384	372
July	0	331	1573	469	2613	3200	3680	0	580
August	0	1240	170	4320	1800	3760	0	3267	4800
September	0	0	0	0	418	820	1307	960	0
October	0	1413	1680	2360	3600	1020	594	736	313
November	0	0	0	907	0	540	540	0	0
December	0	0	0	580	0	787	773	376	933
January	0	457	0	0	1300	0	0	391	560
N WW	a	b	c	d	e	f	g	h	i
May	840	0	384	457	0	0	0	0	109
June	1088	421	869	3160	0	0	1140	3400	1320
July	1680	0	613	0	0	720	2880	1933	2400
August	704	0	1627	2496	288	457	860	3520	4640
September	1760	1760	1627	1386	1440	2016	1147	2640	3480
October	3520	960	613	1350	0	3816	0	637	1380
November	760	0	0	0	0	0	2640	800	0
December	590	124	0	440	1600	784	4400	1013	2000
January	1307	331	0	0	0	0	0	160	560

WE: the Washidu East quadrat; WW: the Washidu West quadrat (please see [1]). Scientific names of Dictyostelia species: *P. pallidum*: *Polysphondylium pallidum*; *D. purpureum*: *Dictyostelium purpureum*; and *P. violaceum*: *Polysphondylium violaceum*. For calculation of $\Re(s)$, see the main text. N is number of cells per 1 g of soil. Species names for Dictyostelia represent the corresponding values. a - i indicate the indices of the point quadrats. Red indicates $\Re(s)$ values of species that were approximately integral numbers greater than or equal to 2.

system. We now consider situations in harmonic neutrality. $\Re(s) > 2$ is an indicator of adaptation beyond the effects of fluctuation from individuals with harmonic neutrality. Also note that $\mu(n)$ represents the bosonic 1 with an even number of prime multiplications, the fermionic -1 with an odd number of multiplications, or 0 as the observant, which can be divided by a square of prime. This occurs when two quantized particles interact. Note that in about 1400 CE, Madhava of Sangamagrama proved that

$$\sum_{n:odd} (-1)^{(n-1)/2} / n = \pi/4.$$

This means that the expected interactions of a large number n of fermions can be described as $\pi/4$. The interaction of the two particles means multipli-

cation by 2, which results in $\pi/2$, as discussed in the next subsection where an imaginary axis is rotated from a real axis by the angle of $\pi/2$.

3.3. Introducing $\Im(s)$ explains adaptation/disadaptation of species

Next, we need to consider $R = T$ theory, Weil's explicit formula, and some algebraic number theory to define $\Im(s)$ precisely. $R = T$ theory is based on an ordinary representation of a Galois deformation ring. If we consider the mapping to T that is shown below, they become isomorphic and fulfill the conditions for a theta function for zeta analysis. Let $(s \in \mathbb{C}, D \in \mathbb{C})$, where \mathbb{C} is complex. First, we introduce a small s that fulfills the requirements from a higher-dimensional theta function. Assuming $\mathbb{H}, \mathbb{C}, \mathbb{R}, \mathbb{R}_+, \mathbb{R}_\pm$ as a higher-dimensional analogue of the upper half-plane, a complex $\prod \mathbb{C} = \frac{1}{k^s \zeta}$, $[\prod \mathbb{C}]^+ = \{z \in \mathbb{C} | z = \bar{z}\} / T_H$ (Hecke ring, $R = T$ theorem), $|\Im(s)|$ dual with $|\Re|$ [109], $\ln |\Im(s)|$, s could be set on \mathbb{H} and $\ln |\Im(s)| = \ln(|D|^{E(\Sigma N)}) = E(\Sigma N) \ln |D|$ is a part of $\Re(s) = b \ln |D|$. Thus, $\mathbb{H} \subseteq \mathbb{C} \supseteq \mathbb{R} \supseteq \mathbb{R}_\pm \supseteq \mathbb{R}_+^*$, and the functions described here constitute a theta function. The series converges absolutely and uniformly on every compact subset of $\mathbb{R} \times \mathbb{R} \times \mathbb{H}$ [70], and this describes a $(3 + 1)$ -dimensional system. This is based on the $R = T$ theorem and Weil's explicit formula (correspondence of zeta zero points, Hecke operator, and Hecke ring); for a more detailed discussion, see [109, 98, 113, 46]. Since b is real, $\Re(s) = b \ln |D|$ and $\Im(s) = b \arg D$. Thus, $\Re(s)$ is related to the absolute value of an individual's fitness, and $\Im(s)$ is the time scale for oscillations of D and is the argument multiplied by the b scale. Therefore,

$$\frac{\partial \Re(s)}{\partial t} = b \frac{1}{|D|} \frac{\partial |D|}{\partial t}, \quad (26)$$

$$\frac{\partial \Im(s)}{\partial t} = b \frac{\partial \arg D}{\partial t}. \quad (27)$$

When $0 < \Re(s) < 1$ and $|D'| > 0$, $\Re(s) \sim 1$ and we usually have harmonic neutrality. This case was often prominent in the Dictyostelia data. When $0 < \Re(s) < 1$ and $|D'| < 0$, $\Re(s) \sim 0$ and we usually have Möbius neutrality. When $1 < \Re(s) < 2$, the population/species can diverge when $\Im(s) = T$, that is, when it equals the imaginary part of a nontrivial zero of ζ for $w = s - 1$ as . Thus, the population/species can diverge when $\arg D = T/b$. We also note that

$$D = e^{\frac{s}{b}} = e^{\frac{\Re(s)}{b}} \left(\cos \frac{\Im(s)}{b} + i \sin \frac{\Im(s)}{b} \right), \quad (28)$$

so $\Im(s) \sim \pm m(\pi/2)b$ for quantization (compactification of m , which is a natural number; generally, quantization refers to the procedure of constraining something from a continuous state to a discrete state; $\pi/2$ value is calculable from Madhava's equation described earlier), assuming that the distribution of population/species numbers is in equilibrium and is dependent on interactions between them, as described in the previous subsection; thus, $|D| = e^{\Re(s)/b}$. With the Riemann-von Mangoldt formula [104], the number of nontrivial zero points $N(T)$ is

$$N(T) = \frac{T}{2\pi} \log \frac{T}{2\pi} - \frac{T}{2\pi} + O(\log T), \quad (29)$$

so that $T \sim 2\pi e^{2\pi N(T)/T+1}$. Note that from Stirling's approximation, $N(T) = \ln n! \approx n \ln n - n$, indicating that the number of species is equal to the sum of the relative entropies. On the other hand, $T = \pm m(\pi/2)b$. Therefore, for populations/species as a whole, $|D|^{E(\Sigma N)} = e^{m\pi\Re(s)\Sigma N/2T}$. Since the $|D|^{E(\Sigma N)}$ axis and the $T/\arg D$ axis are orthogonal and the scale of the latter is 2π times that of the former, $|D|^{E(\Sigma N)} \approx |T|$ (Table 2) gives a good fit to a highly adaptive population/species growth burst or collapse for an entire population or species and m can be calculated as

$$m = \frac{1}{\Re(s)E(\Sigma N)}(4N(T) + \frac{2T}{\pi}(\ln 2\pi + 1)). \quad (30)$$

If we set a particular unit space for calculation of population density, $\Im(s) = e^{\Re(s)E(\Sigma N)/b}$ is obviously a scale invariant for the case of species, where $\Re(s)$ is a scale invariant to system size, b is the order of the ratio of the sum of population densities of a particular species to the number of patches, and $E(\Sigma N)$ is the ratio of the sum of the population densities to the number of patches. For a given population, if b is the order of the population density of a particular patch, it is also a scale invariant to the sampling size, assuming that a sufficiently large number of samples are collected. Nontrivial zeros of ζ are *prime states* (those related to prime numbers), and they are indicators of imminent growth bursts or collapses of the population/species. Note that ζ can also be expressed as follows [81]:

$$\zeta(s) = 2^s \pi^{s-1} \sin \frac{\pi s}{2} \Gamma(1-s) \zeta(1-s) = 2^s \pi^s \sin \frac{\pi s}{2} \frac{1}{\Gamma(s) \sin \pi s} \zeta(1-s). \quad (31)$$

To avoid a discontinuity at a zero of ζ , $\Re(s)$ is $3/2$ ($w = s - 1 = 1/2$) or an integer. Zero points of ζ thus restrict both $\Re(s)$ and $\Im(s)$ to a particular point. Note that T consists of the imaginary parts of the ζ zeros,

which are not integers themselves in the quantization. This model is found to be consistent with the results for some species, as shown in red in Table 1: $(\Re(s), \Im(s) \approx T, m) = (3.078, 14.99, 0.01003), (4.942, 38.74, 0.01723), (2.056, 275.5, 2.994), (2.8795, 13.80, 0.009451), (2.1411, 115.9, 0.05094), (2.9047, 13.93, 0.004941)$. Thus, this model gives a logical explanation for the observed quantization in some situations for the Dictyostelia species regarding $O(\log T)$, and for a population, the data do not seem to be at a zero point, according to the $\Im(s)$ value. Except for the case $(2.056, 275.5, 2.994)$, they are in a situation similar to a Bose-Einstein condensate; this is discussed in later sections.

There is another way of describing quantization. First, think of the tube zeta function $\tilde{\zeta}_A(s) := \int_0^\delta t^{s-N-1} |A_t| dt_t$ as before. Think of $r \rightarrow +\infty$ and then

$$\int_{1/r}^\delta t_t^{\dim_B A - N - 1} |A_t| dt_t \sim \text{res}(\tilde{\zeta}_A, \dim_B A) \ln r \quad (32)$$

[57]. We can set an average Minkowski content as

$$\tilde{\mathcal{M}}^{\dim_B A}(A) := \lim_{r \rightarrow +\infty} \frac{1}{\ln r} \int_{1/r}^\delta t_t^{\dim_B A - N - 1} |A_t| dt_t. \quad (33)$$

From the Lemma 2.4.7. for [57],

$$\tilde{\mathcal{M}}^{*s}(A) = \begin{cases} 0 & (\text{for } \Re(s) > \overline{D}_{av}) \\ +\infty & (\text{for } 0 \leq \Re(s) < \overline{D}_{av}) \end{cases}, \quad (34)$$

$$\tilde{\mathcal{M}}_*^s(A) = \begin{cases} 0 & (\text{for } \Re(s) > \underline{D}_{av}) \\ +\infty & (\text{for } 0 \leq \Re(s) < \underline{D}_{av}) \end{cases}, \quad (35)$$

where D_{av} is an average Minkowski dimension. When $\dim_B A$ exists, $D_{av} = \dim_B A$ (Proposition 2.4.9. of [57]) and as $\Re(s) = \dim_B A \rightarrow D_{av}$, $\tilde{\mathcal{M}}^s(A)$ will converge to $\lim_{r \rightarrow +\infty} \frac{1}{\ln r} \int_{1/r}^\delta t_t^{\dim_B A - N - 1} |A_t| dt_t = F(t)$, independent of δ, r .

Thus quantization related with w occurs.

Similarly, think of the tube zeta function of second kind $\tilde{\zeta}_{2A}(s) := \int_0^\delta t_t^{s-N} |A_t| dt_t$ as before. Think of $r \rightarrow +\infty$ and then

$$\int_{1/r}^\delta t_t^{\dim_B A - N} |A_t| dt_t \sim \text{res}(\tilde{\zeta}_{2A}, \dim_B A) \delta. \quad (36)$$

We can set an average Minkowski content as

$$\tilde{\mathcal{M}}_2^{\dim_B A}(A) := \lim_{r \rightarrow +\infty} \frac{1}{\delta} \int_{1/r}^{\delta} t_t^{\dim_B A - N} |A_t| dt_t. \quad (37)$$

Then,

$$\tilde{\mathcal{M}}_2^{*s}(A) = \begin{cases} 0 & (\text{for } \Re(s) > \overline{D}_{av}) \\ +\infty & (\text{for } 0 \leq \Re(s) < \overline{D}_{av}) \end{cases}, \quad (38)$$

$$\tilde{\mathcal{M}}_2^s(A) = \begin{cases} 0 & (\text{for } \Re(s) > \underline{D}_{av}) \\ +\infty & (\text{for } 0 \leq \Re(s) < \underline{D}_{av}) \end{cases}, \quad (39)$$

where D_{av} is an average Minkowski dimension. When $\dim_B A$ exists, $D_{av} = \dim_B A$ and as $\Re(s) = \dim_B A \rightarrow D_{av}$, $\tilde{\mathcal{M}}_2^s(A)$ will converge to $\lim_{r \rightarrow +\infty} \frac{1}{\delta} \int_{1/r}^{\delta} t_t^{\dim_B A - N} |A_t| dt_t = F(t_t)$, independent of δ, r . Thus quantization related with s also occurs. In these ways, quantization is an expected outcome of Minkowski components, for both w and s .

Also note that here we assume continuity of functions or the existence of $\dim_B A$, which is likely to be held in natural systems. This is a mere description, and not a mathematical proof.

Now consider $\text{res}(\tilde{\zeta}_A, \dim_B A) = \text{res}(\tilde{\zeta}_{2A}, \dim_B A)$. Then, as $\delta \rightarrow r$,

$$\frac{\tilde{\zeta}_{2A}}{\tilde{\zeta}_A} \sim \frac{r}{\ln r} \sim \pi(r) \quad (40)$$

where $\pi(r)$ is the prime counting function as r is sufficiently large. Thus r can be converted to the number of quantizations possible, and larger it becomes, the closer it approaches the characteristics of primes and quantization by primes is thus achieved. Next, consider an absolute zeta function:

$$\zeta_{\mathbb{G}_m/F_1}(s) = \frac{s}{s-1} = \frac{s}{w}, \quad (41)$$

when $\mathbb{G}_m = GL(1)$. The tube zeta functions acting on the denominator ($\tilde{\zeta}_A$) and the numerator ($\tilde{\zeta}_{2A}$) convert the absolute zeta function to the prime counting function. The number of primes is thus calculable from F_1

When $\Re(s) > 1$ and $|D|' > 0$, the population/species distribution is always structured without neutrality, since there is no zero point. On the other hand, when $\Re(s) > 1$ and $|D|' < 0$, $\Re(s) \sim 1$ and harmonic neutrality usually

Table 2: T , $\Im(s)$, p , and $|N(p)|$ values.

T	WE <i>P. pallidum</i>	WE <i>D. purpureum</i>	WE <i>P. violaceum</i>	WW <i>P. pallidum</i>	WW <i>D. purpureum</i>	WW <i>P. violaceum</i>	$\Im(s)$	WE <i>P. pallidum</i>	WE <i>D. purpureum</i>	WE <i>P. violaceum</i>	WW <i>P. pallidum</i>	WW <i>D. purpureum</i>	WW <i>P. violaceum</i>
Mar							May						
June		147.4228	30.4249				June	8.1822	148.6187	31.1005			
July				40.9187			July				39.3062	5.3115	174.5203
August				21.0220	14.1347		August				22.6267	13.7962	2.4878
September	21.0220	14.1347		52.9703	116.2267		September	23.2403	14.9897		2.4101	53.1153	115.8800
October	48.0052	37.8962					October	43.0793	38.7434		2.0958	22.0635	2.4764
November	14.1347		275.5875				November	7.7262	15.3773		275.5449		
December							December						
January							January						
Mar							Mar						
June	1	2/0	7				June	1	1	1	1	1	1
July				17	1	317	July	1	1	1	1	1	1
August				3		1	August	1	1	1	1	1	1
September	3		4	31	100	4	September	1	1	1	1	1	1
October	23	13	3	3	2	2	October	1	1	1	1	1	1
November	1	2	377				November	1	1	1	1	1	1
December							December						
January							January	1	1	1	1	1	1
Mar							Mar						
June	0.938	0.946	0.863				June	1.011	0.885	1.017	1.020	0.959	1.059
July				0.884	1.000		July	0.973	0.993	0.989	0.997	0.991	0.991
August				0.941	0.971	0.900	August	0.962	0.965	0.959	0.987	0.981	0.992
September	0.939	0.941	0.874		0.922	1.000	September	1.023	1.012	1.010	0.982	1.007	1.008
October	0.979	0.957	0.946		0.962	0.962	October	0.981	0.988	1.000	1.002	1.000	1.001
November	0.946						November	0.969	0.968	0.969	0.969	0.969	0.968
December							December	0.984	0.984	1.000	0.999	0.988	0.970
January							January	0.994	1.008	1.008	0.999	1.037	1.037

WE: the Washidu East quadrat; WW: the Washidu West quadrat (please see [1]). Scientific names of Dictyostelia species: *P. pallidum*: *Polysphondylium pallidum*; *D. purpureum*: *Dictyostelium purpureum*; and *P. violaceum*: *Polysphondylium violaceum*. T consists of the theoretical imaginary parts of the Riemann ζ zero points corresponding to p and $\Im(s) = |D|^{E(\Sigma N)}$. a - i indicate the indices of the point quadrats. The $T/\Im(s)$ of populations are not shown because the $\Im(s)$ are so small that T and $\Im(s)$ do not correspond to each other. In this case, p is set at 1. For calculation of p and $|N(p)|$, see the main text. Blank values are undefinable. Red indicates species for which $|N(p)|$ was approximately 2/3.

occurs. This is true for Dictyostelia. Usually, $D_k \sim 1$ is the equilibrium state. Therefore, populations/species reach either Möbius neutrality or harmonic neutrality.

We note that if we assume $p_k = f_s(k)$, the information entropy ($I_e = -\sum p(n) \ln(p(n))$), which is the same as the Shannon index, can be written as

$$I_e = \sum p_k (s \ln k + \ln |\zeta|). \quad (42)$$

That is, the expected $p_k = \text{constant}$ output of information entropy for the k th population/species is $s \ln k + \ln |\zeta|$. Therefore, maximizing $|\zeta|$ for $s \sim 1$ is the expected result from maximizing the information entropy. The populations/species thus usually fluctuate for $s \sim 1$. If there is no force against entropy, this is the expected future. Additionally, as zero points of ζ are approached, information is minimized and approaches negative infinity; this is the opposite to what occurs when $s \sim 1$, and it indicates ordering/domination. The concept described here is analogous to $H = \lambda - \Phi$ in [3], where H , λ , and Φ are population entropy, growth rate, and reproductive potential, respectively. That is, λ is analogous to $p_k s \ln k$, and the reproductive potential is analogous to $-p_k \ln |\zeta|$.

Interestingly, according to [35],

$$\int_0^T |\zeta(\frac{1}{2} + it)|^2 dt \approx |T \ln |T||, \quad (43)$$

$$\int_0^T |\zeta(\Re(w) + it)|^2 dt \approx |T\zeta(2\Re(w))|. \quad (44)$$

Since $|T| \approx e^{\Re(w)/b}$,

$$\frac{\int_0^T |\zeta(\frac{1}{2} + it)|^2 dt/T}{\int_0^T |\zeta(\Re(w) + it)|^2 dt/T} \approx \left| \frac{\Re(w)}{b\zeta(2\Re(w))} \right| \approx \left| \frac{\Re(w)}{b} \right| (\Re(w) \gg 1) \quad (45)$$

gives an indicator of the distance from the speciation line on $\Re(w) = 1/2$. Since $\zeta^2 = \sum_{n=1}^{\infty} \frac{d(n)}{n^s}$, ζ^2 is the sum of (the probability that an individual in the top populations/species replaces an individual of the n th population/species) \times (the number of combinations/entanglements, assuming the constituents are equivalent). This represents the expected number of entanglements and approaches 1 when the community progresses far beyond the speciation phase. Ideally, the development of a community begins when $\frac{\Re(s)}{b} = 0$ and eventually arrives at the expected state.

A virtual world of adaptation of a particular species/population is thus represented on a purely imaginary axis of small s . To calculate the synthetic fitness, $(s - 1)^n$, simply evaluate $[L_M, \partial^*] = i\bar{\partial}$, where M is the Kähler manifold of an $(s - 1) \setminus \{s = 1\}$ space and L_M is the Lefschetz operator [85]. The hard Lefschetz theorem indicates whether the dimension of the space is decreasing or increasing with n . The Hasse zeta function is

$$\zeta_{\mathbb{Z}[T]}(s) = \prod_p (1 - p^{1-s})^{-1} = \zeta(s - 1), \quad (46)$$

which is the zeta function of $w = s - 1$ when $\mathbb{Z}[T]$ is a one-variant polynomial ring.

3.4. Interpretations of $\Im(s)$ and $\Re(s)$ in group theory regarding p -Sylow subgroups and their topological nature

In the previous sections, we became able to calculate primes p from corresponding $\Im(s)$ values in species. We could also calculate $\Re(s)$ values, and this would exactly be l_i values introduced in Sylow theorems in the Introduction when it is an integer. We justify these ideas in what follows.

When $p = 2$, a prime number p can count the number of interactions as 2; an equality (non-interactive state, 0_G) or a self-interaction (1_G). In all primes, symmetries ensure that a species only involves an equality (non-interactive

state, 0_G) or a self-interaction (1_G) as a whole and no other subgroups emerge within the p -numbered species, at least on characteristic space-time scales of interest, because an order of a subgroup p is a prime. This ensures the stabilized identity of a species. Next, recall $\mathfrak{R}(s)$ is a fractal dimension in our model for species. In the fractal structure, the order of p -Sylow subgroup should be p^l , when $l = \mathfrak{R}(s)$.

Thus, we are able to characterize a computation method for p, l for the ‘‘Sylow theorems’’ introduced earlier. In this sense, an element of a community (group) G is the number of different interaction modes in p -numbered species with directionality from a species to another, as deduced from the character of the mathematical group. A nilpotent group means after finitely many steps, all interactions finally result in the self-interaction (1_G) of constitutes (preservation of the identity of interactions) as doing something good for themselves. This logic characterizes a species concept based on p -Sylow subgroups, established among interaction mode of the species, not merely based on a particular species. This discussion leads to a species concept relating to a category theory in mathematics.

Now we further expand the interpretations with topological theory. Regarding a space described by s, w of species k is locally compact, let us set a function $f : Q \rightarrow R$ where Q, R are compact Riemann surfaces derived from the locally compact spaces at the population and species level, respectively. Let us also neglect the case for $k = 1$ so as to ensure the function f is regular. With a fractal dimension l , Q for each species has a single ramification with a ramification index of l . Next, let f be a covering function with a degree of $E(\Sigma N)$ at a complement of $f^{-1}(f(Q_r))$ where Q_r is a set of ramification points. Introducing a genus number $g(Q), g(R)$ results in the Riemann-Hurwitz formula [37]

$$g(R) - 1 = \frac{1}{2} \sum_{i=1}^g (l_i - 1) + E(\Sigma N)(g(Q) - 1). \quad (47)$$

Equating genus number $g(Q), g(R)$ for $\mathfrak{R}(s)$ of populations and species as isolated singularities, and $g(Q) - 1 = w_Q$ (that is, w_Q is averaged fitness of individuals, and $E(\Sigma N)(g(Q) - 1)$ is fitness of population as a whole), we can obtain the modified Price equation introduced earlier:

$$w_R = \mathfrak{R}(s_Q) - 1 + \mathfrak{S}(s_Q), \quad (48)$$

where $\mathfrak{R}(s_Q) - 1 = \frac{1}{2} \sum_{i=1}^g (l_i - 1)$. For multiple species in a community, we can also sum w_R to determine community fitness if we can collect all the

species involved. Since l is the number of conjugates of p_i -Sylow subgroup and equals the order of G/N_i in species i , it should be a prime given that G also has stable identity observed from a p_i -Sylow subgroup and no subgroup separates from G . If $p \neq 2$, $\Re(s_Q)$ is an integer and fulfills the foregoing logic. In the case of $p = 2$, $\Re(s_Q) - 1 = \frac{1}{2}$ and it seems to be on a hypothetical line of zero points of Riemann zeta function. We will show later in our biological model that the Riemann hypothesis is likely to be true because we have many assumptions in our lines of logic compared with mathematical situations. This expansion further clarifies that our w_R value is a sum of an average contribution from w_Q values and further contributions from fractal structures: w_Q , which invests fitness advantage in the layer above the original layer, e.g., species and population.

3.5. Selberg zeta-function and Eisenstein series reveal Maass wave form as a function of probability of population number distribution and genetic information

Once we have obtained the small s for a system, we then apply the automorphic L -function to calculate the Eisenstein series. This allows us to understand the relation of small s to the diffusion equation in neutral theory and to obtain further information about the prime closed geodesics, which are used to further analyze the intra-population/species interacting mode [68]. The prime closed geodesics on a hyperbolic surface are primitive closed geodesics that trace out their image exactly once. The expression prime obeys an asymptotic distribution law similar to the prime number theorem. For this application, we must discriminate between the discrete spectrum and the continuous spectrum of a Selberg zeta-function. We can then proceed to calculate the Eisenstein series that corresponds to the discrete spectrum.

The Selberg zeta function is defined by

$$\zeta_{\Gamma}(s) = \prod_p (1 - N(p)^{-s})^{-1}, \quad (49)$$

where $N(p)$ is a norm of prime closed geodesic. The determinant of the Laplacian of the complete Selberg zeta-function is

$$\det(\Delta, s) = \det_D(\Delta - s(1 - s)) \det_C(\Delta, s), \quad (50)$$

$$\det(\Delta, s) = s(1 - s), \det_C(\Delta, s) = \hat{\zeta}(2s), \quad (51)$$

where $\hat{\zeta}(s) = \pi^{-s/2}\Gamma(s/2)\zeta(s)$, and D and C denote discrete and continuous spectra, respectively [68]. It is evident both in populations and species that the discrete spectrum dominates the continuous spectrum by $\sim 10^3$ (populations) or $\sim 10^{263}$ (species). When d is assumed to be the dimension of a compact oriented hyperbolic manifold, the number of prime closed geodesics in a Selberg zeta-function $N'(T)$ is [19]

$$N'(T) \sim \frac{e^{(d-1)T}}{(d-1)T} (T \gg 1). \quad (52)$$

Table 3 lists the calculated determinants, Magnus expansion/Eisenstein series $E(s)$, and other parameter values. $E(s)$ is defined as follows:

$$E(s) = \sum_{n=-\infty}^{\infty} a_n(s) e^{2\pi i n \Re(s)}, \quad (53)$$

$$a_0(s) = \mathfrak{S}(s)^s + \frac{\hat{\zeta}(2s-1)}{\hat{\zeta}(2s)} \mathfrak{S}(s)^{1-s}, \quad (54)$$

$$a_n(s) = \frac{2|n|^{s-1/2} \sqrt{\mathfrak{S}(s)} K_{s-1/2}(2\pi|n|\mathfrak{S}(s))}{\hat{\zeta}(2s)} \sigma_{1-2s}(|n|), \quad (55)$$

where K is the modified Bessel function of the second kind, and σ is the divisor function [68].

In the diffusion equation of the neutral theory of population genetics [45],

$$\frac{\partial \phi}{\partial t} = \frac{1}{2N} \Delta u = \frac{\lambda}{2N} u, \quad (56)$$

where λ and u are an eigenvalue and an eigenfunction, respectively, and $\phi = N_k/E(\Sigma N)$. Let a manifold M be constituted by $s \setminus \{s = 1\}$ (non-degenerate as shown earlier). If we let $f_M = u/(2N_k)$, then f_M is a Morse function because the Hessian of f_M is assumed to be nonzero. We would like to know $\Delta f_M = 0$ to analyze the conditions under which the system is at equilibrium. When $f(x)$ is a function of genetic information, $u = f(x)\phi = E(s)$ and the Dirac operator is $D_{irac} = \sqrt{1/4 - \Delta} = \sqrt{1/4 - s(1-s)} = s - 0.5$. In adapted/collapsed positions of the Riemann ζ zero values, the most promising virtual adaptation of $|D|^{E(\Sigma N)}$ is on the purely imaginary axis of the Dirac operator if the Riemann hypothesis is true. Indeed, in our physical model, the hypothesis is very likely to hold, as will be discussed below.

3.6. *Geodesics of zeta-functions elucidate the mode of interaction within the systems and its expansion*

Let E be an elliptic curve over a rational \mathbb{Q} of a \mathbb{Q} -approximated conductor $N_c = \ln N_k / \ln k = z - 1$, defined above in the first part of the Results section when discussing the Price equation. Let p be the corresponding prime for each $|D|^{E(\Sigma N)}$ value, including $p = 1$ when $\pi(|D|^{E(\Sigma N)}) = 0$, and consider the Hasse-Weil L -function on N_c/\mathbb{Q} :

$$L(s, E) = \prod_p L_p(s, E)^{-1}, \quad (57)$$

$$L_p(s, E) = \begin{cases} (1 - a_n p^{-s} + p^{1-2s}), & \text{if } p \nmid N_c \text{ or } p = 1 \text{ when } N(p) \neq 0, \\ (1 - a_n p^{-s}), & \text{if } p(\neq 1) \parallel N_c \text{ when } N(p) \neq 0, \\ 1, & \text{if } p^2(\neq 1) \mid N_c \text{ when } N(p) \neq 0 \text{ or } N(p) = 0. \end{cases} \quad (58)$$

Note that an ideal $L_p(s, E)$ is a conductor of $L(s, E)|\mathbb{K}$ when \mathbb{K} is a finite extension of a rational \mathbb{Q} . When $L_p \nmid \infty$, the global Artin conductor $L(s, E)$ should be 1 or -1 , and the system will fluctuate [70]. Note that if $\Re(s) > 2$, $L(s, E)$ converges as expected from the border between populations and species [43].

Considering that the geodesic $N(p)$ in the Selberg zeta function, the Hasse-Weil L -function on N_c/\mathbb{Q} is

$$\zeta_\Gamma(s) = \prod_p (1 - N(p)^{-s})^{-1}. \quad (59)$$

In the observed data for Dictyostelia (Table 2), in most cases, $N(p)^{-s} = a_n p^{-s} - p^{1-2s}$, and $|N(p)|$ is either 1 or $2/3$ for the first order. The 95% confidential intervals are $0.93 \pm 0.03/0.66 \pm 0.01$ for species and 0.991 ± 0.007 for populations. A smaller a_n indicates a larger effect, and according to Table 3, in nonevolving situations, the dominant species is independent of the covariance of the Price equation, as is often the case for observed species data, for which a_0 is the smallest coefficient of the Eisenstein series. For populations, $|a_1|$ is always the smallest. When the smallest coefficients depend on $\Re(s)$, the first orders are the smallest for almost all cases, except as discussed above. It also may occur when $p \parallel N_c$, $|N(p)| = p$ or $2/3 * p$, and in this case, the population/species will be in a branch cut. N_c is thus related to the information of the lower hierarchy as N_k and to that of the

upper hierarchy as k . If the ratio of their logarithms is a multiple of p , the branch cut becomes apparent.

Next, let us assume $Q = [q_a, q_b, q_c] = q_a X^2 + q_b XY + q_c Y^2, -q_d = q_b^2 - 4q_a q_c$. This assumption implies an interaction mode with the complete parameters of the subpopulations X and Y in a particular population/species. The Hurwitz-Kronecker class numbers $H(q_d) = \Sigma 1/w_Q$ in a Jacobi theta function, which is a shadow of the Eisenstein series $E(s)$, should be $|N(p)|$, according to the trace formula [117]. Now, consider q_d modulo 4 for the symmetrical case $q_a = q_c$. Unless $Q = [q_a, 0, q_a]$ or $[q_a, q_a, q_a]$ with $w_Q = 2$ or 3 , w_Q should be unity [118]. If $H(q_d) = 2/3$, then $q_a = 3$ and $q_b = 0$ because q_a is an integer. Therefore, there is no heterointeraction between the subpopulations. The $|N(p)| = 2/3$ mode thus represents a noninteracting mode. Furthermore, we exclude the cases with 2 or 3 zeros among q_a, q_b, q_c because we require proper subpopulations as X, Y . $|N(p)| = 1$ therefore implies an interacting mode with $q_a = q_b = q_c = 3$ or a noninteracting mode with $q_a = q_c = 2, q_b = 0$. Below, we will show that the former is necessary. When the infinite generation ring $A_r \subset C$ is $A_r = Z[\{1/2\} \cup \{1/q_m \mid q_m \equiv 3 \pmod{4}\}]$, the Hasse zeta

$$\zeta_{A_r}(s) = \prod_{p \equiv 1 \pmod{4}} (1 - p^{-s})^{-1}$$

has a possible analytic continuation in $\Re(s) > 0$ and $\Re(s) = 0$ is a natural boundary [56]. Since p in Table 2 is either 1 mod 4 or $[\{1/2\} \cup \{1/q_m \mid q_m \equiv 3 \pmod{4}\}]$, the 1 mod 4 part represents a characteristic ζ with Möbius neutrality. The $[\{1/2\} \cup \{1/q_m \mid q_m \equiv 3 \pmod{4}\}]$ part represents an infinite generation ring of the system; it has the property that a certain combination of minimum spaces are not isomorphic to each other, representing an asymmetry of the system, which is approaching a singularity (Bott-Shapiro Lemma; [66]). It is notable that the $|N(p)| = 1$ case demonstrates $L_p \nmid \infty$, and the $|N(p)| = 2/3$ case demonstrates $L_p \mid \infty$; therefore, they represent discontinuous and continuous courses, respectively [70]. In other words, the 1 mod 4 case is in the unique factorization domain on \mathbb{H} with oscillative imaginary dimension, and the 3 mod 4 case is not because of the lack of oscillative dimension. From Table 1, Table 2, and [1], it is observed that the 3 mod 4 case is described as being adapted stages, and the 1 mod 4 case is nonadapted stages. The 2 cases are at ramification and likely to be involved in Bose-Einstein condensates with maximum T_s values, as described in later sections. Now consider an odd prime p . The fields generated by p have an

imaginary part when $p \equiv 1 \pmod{4}$, but not when $p \equiv 3 \pmod{4}$. Since, in our model, the imaginary part i is related to oscillation, $p \equiv 1 \pmod{4}$ is still in the world of fluctuation, and $p \equiv 3 \pmod{4}$ is in a directional world. We use statistical mechanics to expand this interpretation in what follows.

Note that a quartic potential $V_p = \phi > 0$ represents a state that has already occurred in $\Re(s) > 0$, while $V_p < 0$ can represent a future state with a normally divergent Eisenstein series. This is only converged/predictable when $[V_p = -\phi, \Re(s-1) \approx -1/(3\phi)$ and $\Im(s-1) \approx \pm e^{-1/(3\phi)}$] (note that it is bosonic; [61]). [11] showed that three-dimensional minimal models are not unique, but they are unique at the level of a derived category. For additional support for this idea, see [87], in which the variations in multiscale bootstrap analysis are expanded from positive to negative values, rendering the Bayesian nature of bootstrap analysis in the plus values of $\Re(s)$ converted to frequentist probability in the minus values of $\Re(s)$ as in [87]. Consider the situation when $s = w + 1$. Because our model assumes a zero-sum patch game with neutrality as the null hypothesis, bootstrapping is an analog of the situation, especially when $\Re(s) > 0$. With this reversing of curvature, the expected future of $\Im(s)$ as a Bayesian principle could be converted to a frequentist principle predicting further in the future. More specifically, the predictable points are usually close to the real axis, and the trivial zeros of the Riemann ζ ($-1/3\phi = -2l_s, \Im(s-1) = 0$) can be used to predict the adaptation/disadaptation of the population/species of interest. In Washidu East, this can be observed during June for *P. pallidum* ($-1/3\phi = -2.044$, adaptation in next month) and during September for *D. purpureum* (-4.148 , disadaptation in next month); in Washidu West, it can be observed during July for *D. purpureum* (-1.954 , disadaptation in next month) and during October for *P. violaceum* (-3.830 , disadaptation in next month). For simplicity, consider the Hurwitz zeta function:

$$\zeta(w, k) = \sum_{n=0}^{\infty} \frac{1}{(k+n)^w}. \quad (60)$$

For any k , $-\zeta(w, k)$ with a negative w value is equal to $\frac{B_{-w+1}(k)}{-w+1} = \int B_{-w}(k) dk + C_B$, where $B_{-w}(k)$ is a Bernoulli number and C_B is a constant of integration. That is, for any $-w$ of a positive even number, it becomes 0. Summing all values with differing k from 1 to the number of population/species, it is still 0. This means for any $-w$ of a positive even number, the integrated

output of all the interactions from all the population/species can be represented as $|\zeta(w, k)| = 0$ and it means population burst/collapse of the population/species. Hence why we can deduce the outcome of the future from negative even w values.

In this sense, when there is zero variation, the bootstrapping process becomes machine learning [88] and it is analogous to measurement. Since $\Re(s - 1) = 0$ ($\Re(s) = 1$ for observer $k = 1$ in population) is a natural boundary of the system ζ , harmonic neutrality determines what types of behavior can be observed in the system. When two randomly selected integer constitutes are disjoint, the probability is $1/\zeta(2) = 6/\pi^2$. Distributing this to the positive and negative $\Re(s - 1)$ planes results in a probability of $3/\pi^2$. The probability of being an observer, which corresponds to the nondisjoint case, is therefore $1 - 6/\pi^2$. That is, the probabilities for $\mu(n) = 0, 1, -1$ are $1 - 6/\pi^2, 3/\pi^2, 3/\pi^2$. This case is very likely to occur in our statistical model and thus for nontrivial zeros of ζ , $\Re(s - 1) = 1/2$ [21]. Furthermore, the absolute Riemann hypothesis can be rewritten as follows:

$$\zeta_h(s, \rho) = \prod_{\alpha} \zeta_h(s - \alpha)^{\text{mult}(\alpha)} = 0, \infty \Rightarrow \Re(s) \in \frac{1}{2}\mathbb{Z}, \quad (61)$$

where ζ_h is an absolute zeta function and $\alpha \in \mathbb{R}i$. In our biological model without considering future ($\Re(s) > 0$), $\zeta_h(s, \rho) = 0, \infty$ means $s = 0, 1$ and so obviously, this condition is fulfilled.

3.7. Use of statistical mechanics in the model

From the initial presentation, we could demonstrate eigenvalue-like values, eigenfunction-like functions, and interaction modes of the model. However, we can apply statistical mechanical concepts [30, 5] to the dynamics of populations and species to demonstrate their macroscopic phase transitions. For this, we considered distinguishable individuals with Boltzmann statistics and indistinguishable individuals with Bose statistics [5]. Please note that this is not a generalized approach for applying statistical mechanics to ecology; we use it to prove the existence of Bose-Einstein condensation in an adaptive species. Our approach is different from $(1 + 1)$ -dimensional phase transitions and Bose-Einstein condensation, such as was described by [8]. According to the main body of this manuscript, we need more dimensions. Furthermore, our model is based on empirical data, not merely theory; it is not appropriate for living organisms that have significantly high rates of

immigration, and we avoid the difficulties caused by considering dynamics in physical spaces.

As in the unified neutral theory [38, 39] and in the model of a *Dictyostelia* community [1], the number of individuals within a population/species is denoted as N_k . The population has a logarithmic distribution for the rank of the number of individuals k , which is equal to the number of individuals within a population in a particular patch. For species, the average number of individuals of a particular species in a particular patch is calculated, and the distribution is roughly approximated by a logarithm before comparison to a population. Recall that

$$N_k = a - b \ln k. \quad (62)$$

Let us assume a binary condition, in which +1 polarity is defined as the tendency for an individual to replicate and -1 polarity is the tendency to die. In this situation, the probability of +1 polarity determines the increase in the population or species, which is denoted as κ , and -1 polarity determines the decrease, which is denoted as κ' . The overall polarity of each patch is denoted as $\pm h$. Note that the assumption here implies a cooperative increase or decrease in the number of individuals, which is likely to be the case in a biological system. Assuming a canonical ensemble, and assuming that the microstate probability (not microcanonical ensemble) is $P_m = e^{-q_s h}$, the macrostate is the sum of the states with polarity h and $-h$:

$$\kappa = \frac{e^{q_s h}}{Z}, \quad (63)$$

$$\kappa' = \frac{e^{-q_s h}}{Z}, \quad (64)$$

$$Z = e^{q_s h} + e^{-q_s h}, \quad (65)$$

where Z is a partition function, and q_s is a parameter. In this context, the Helmholtz free energy F equals the number of individuals. We also assume $h = F$ for determining the polarity of a patch with F energy. Note that h becomes an intensive parameter within a particular patch of an intra-acting population; note that this is not purely intensive, as is the case in physics. We assume a positive boundary condition, as required by the Lee-Yang theorem, and we assume an infinite volume limit of F [97]. In the theorem, $\Re(h) > 0$ is required by the holomorphic condition in the positive boundary condition, and it holds in this case.

This model was applied to empirical data from both a population and a species to observe the differences between them. Initially, the free energies of independent individuals in a particular environment without time development (this model neglects time) were set to be equal, and for simplicity their sum was set to equal the number of individuals. As an informational analogue with a novel assumption, we set the Gibbs free energy to $G = N_k$ (individuals/g soil; this was not normalized to reflect the spatial scale of the system); the individual living organisms were considered to be the source of free energy. The immigration rate is m_i ; the enthalpy is $H = a - m_i b \ln k$, which was not defined by [36]; the absolute temperature is $T_s = (1 - m_i)b$, which can be converted to the Lagrange multiplier λ_1 [36] = α/N_k [28] = θ/N_k [39] = $1/(N_k T_s)$; and the entropy in this model, the self-information/surprisal [100] of the probability that the first-ranked populations/species interact with the population/species of interest, is simply $\ln k$ for the k th ranked population/species. Note that $\ln k$ is equal to Kullback-Leibler divergence of $\sum_{i=1}^n p_i \ln \frac{p_i}{q_i}$ with $n = 1, p_i = 1, q_i = 1/k$, the interaction probability from the first ranked population/species as stated before. This is different from the information entropy: $I_e = -\sum p(n) \ln(p(n))$, which is the average of the overall information entropy in the system. This idea is similar to that of [23] when the information entropy is $H(p||q) = -\sum p \ln p/q = \sum \ln q$, where p is the probability of the first-ranked population/species, and to that of [5] when the relative entropy $H_{C-G}(\vec{P}) \equiv -\sum P_i \ln P_i/P_{0i} = \sum \ln P_{0i}$, where P_i is the probability of the first-ranked population/species. Note that T_s is an intensive parameter within the observed intra-active community, and it depends on the scaling of N ; it is not purely intensive, as in thermodynamics. Furthermore, the format $N_k = a - b \ln k$ is only achieved when the system is in equilibrium, and mixing the systems does not maintain linearity of the parameters. Based on the immigration rate m_i , the internal energy is $U = (1 - m_i)a$, and the emigrant population (work sent outside the system) is equal to $m_i(a - b \ln k)$. These assumptions reflect that $G = H - T_s S$, $H = U + (\text{emigrant population})$, $\text{entropy} = \ln(\text{the number of states})$, and $N_k = a - b \ln k$. Overall, the number of individuals is analogous to the free energy, and the rank of the population/species can be interpreted as the information represented by the entropy. The temperature T_s is a characteristic parameter of the distribution of the populations/species per gram of soil, which reflects the extent of domination. For constant G and H , as the entropy grows, T_s becomes smaller, analogous to the flow of heat from a warmer to a cooler environment; this is thus anal-

ogous to the second law of thermodynamics. Further, this is analogous to the equation $P = E - ST$ in [3], where P is the free energy (growth rate), E is the mean energy (reproductive potential), T^{-1} is the inverse absolute temperature (generation time τ), and S is the Gibbs-Boltzmann entropy (population entropy $-\tau H$). According to the theory of statistical mechanics [30], $q_s = 1/(1 - m_i)b$, $M_q(T_s) = e^N$, and $\phi(q_s) = q_s F = a/b - \ln k \cdot 1/(1 - m_i)$. The Lagrangian $L = (\textit{kinetic energy}) - (\textit{potential energy})$ of the system is thus $U - (1 - m_i)N_k = T_s \ln k$. The calculations based on actual data for Dictyostelia [1] are shown in Table 4 ($m_i < 10^{-3} \ll 1$ and $G \approx F$). When $N \gg 1$, the correlation function C_q and the spectrum intensity I_q are defined as

$$C_q(t) = C_q(0)e^{-\gamma_q t}, C_q(0) = \frac{4U^2 \kappa \kappa'}{\gamma_q^2}, \quad (66)$$

$$I_q(\omega) = C_q(0) \frac{2\gamma_q}{\omega^2 + \gamma_q^2}, \quad (67)$$

where

$$\gamma_q = 2Uq_s. \quad (68)$$

Note that under low temperatures (temperatures lower than the critical temperature), the correlation function is not unique [97]. The estimated values for $U, T_s, q_s, \kappa, \kappa', \phi(q_s), \gamma_q, \omega$, and $I_q(\omega)$ are presented in Table 4. Compared with populations, species exhibit more stable dynamics, and this is evident in the values we observe for γ_q . Noting that the time scale of the observations is a month, we observe that populations rise and fall over a time scale of approximately a week, while the time scale for species is on the order of approximately three weeks. As expected [1], the climax species *Polysphondylium pallidum* shows less contrast than does the pioneering species *Dictyostelium purpureum/Polysphondylium violaceum*; this is evident in the value of $I_q(\omega)$.

3.8. Adaptation of species

When a system is stimulated by $h = F$, the polarity is

$$M = N_k \cdot Z^{-1}(e^{q_s h} - e^{-q_s h}) = N_k \cdot \tanh(q_s h). \quad (69)$$

For spontaneous polarity, we have $M \neq 0$. Once adapted, the averaged polarities ($M_{mean} = M/N_k$) of the three dominant species, *P. pallidum*, *D. purpureum*, and *P. violaceum*, were larger and showed better adaptation than

Table 4: Statistics of the PzDom model.

WE (population)	$N \approx G \approx F \approx h$	NN	$u \approx a$	$T_b \approx b$	q	κ	κ'	$\theta(q)$	η_q	ω	$I_q(\omega)$	Mmean	W	$E(T)$	T_c	S
WE (population)	$N \approx G \approx F \approx h$	NN	$u \approx a$	$T_b \approx b$	q	κ	κ'	$\theta(q)$	η_q	ω	$I_q(\omega)$	Mmean	W	$E(T)$	T_c	S
May	288	288	1373	913.4	0.0010995	0.6829	0.3475	0.315	3.007	0.5	12244	0.305	943	-29292	2090	-34.3
June	189	189	364	188	0.000949	0.677	0.341	0.305	3.844	0.4	7530	0.31	107	-29744	2090	-21.8
July	1446	1446	4488	1642	0.000918	0.8014	0.4089	0.607	4.284	0.5	474928	0.6024	2439	-1091372	2090	-14.67
August	1072	1072	3205	2467	0.000907	0.8079	0.4095	0.607	4.284	0.5	474928	0.6024	2439	-1091372	2090	-14.67
September	1007	1007	3043	1946	0.000914	0.7349	0.4021	0.518	3.746	0.5	384187	0.5153	2114	-382434	2090	-12
October	1009	1009	3029	1847	0.000904	0.694	0.399	0.507	3.746	0.5	384187	0.5153	2114	-382434	2090	-12
November	1007	1007	3043	1946	0.000914	0.7349	0.4021	0.518	3.746	0.5	384187	0.5153	2114	-382434	2090	-12
December	383	383	750.3	383	0.000924	0.7456	0.4028	0.602	4.022	0.5	5206	0.6029	100	-26942	2090	-34.06
January	301	301	1204	693.3	0.001005	0.7456	0.4028	0.602	4.022	0.5	5206	0.6029	100	-26942	2090	-34.06
WE (<i>P. pallidum</i>)	$N_b \approx G \approx F \approx h$	NN	$u \approx a$	$T_b \approx b$	q	κ	κ'	$\theta(q)$	η_q	ω	$I_q(\omega)$	Mmean	W	$E(T)$	T_c	S
WE (<i>P. pallidum</i>)	$N_b \approx G \approx F \approx h$	NN	$u \approx a$	$T_b \approx b$	q	κ	κ'	$\theta(q)$	η_q	ω	$I_q(\omega)$	Mmean	W	$E(T)$	T_c	S
May	76	76	109	109	0.0009174	0.5	0.5	0	1.886	0.5	3492	0	0	0	1500	-37.3
June	124	124	714.9	130.5	0.0009177	0.6349	0.3477	0.302	3.046	0.5	1614	0.3026	174	-10062	1500	-36.87
July	1252	1252	1329	1329	0.0009151	0.5	0.5	0	1.886	0.5	3492	0	0	0	1500	-37.3
August	1561	1561	2252	0.0009234	0.8	0.7	0.0023	1.886	0.5	1036001	0	20019	0	0	1500	0
September	914	914	300.0	1435	0.0009053	0.8262	0.4148	0.607	4.022	0.5	246264	0.6074	1544	-392303	1500	-18.84
October	1050	1050	1069	1197	0.00091	0.8074	0.4029	0.717	4.13	0.5	44052	0.4148	1435	-20280	1500	-24.81
November	914	914	300.0	1435	0.0009053	0.8262	0.4148	0.607	4.022	0.5	246264	0.6074	1544	-392303	1500	-18.84
December	20	20	180.0	47.4	0.000904	0.8	0.7	0.0023	1.886	0.5	1620	0	0	0	1500	-36.09
January	301	301	1204	693.3	0.001005	0.7456	0.4028	0.602	4.022	0.5	5206	0.6029	100	-26942	2090	-34.06
WE (<i>D. purpureum</i>)	$N_b \approx G \approx F \approx h$	NN	$u \approx a$	$T_b \approx b$	q	κ	κ'	$\theta(q)$	η_q	ω	$I_q(\omega)$	Mmean	W	$E(T)$	T_c	S
WE (<i>D. purpureum</i>)	$N_b \approx G \approx F \approx h$	NN	$u \approx a$	$T_b \approx b$	q	κ	κ'	$\theta(q)$	η_q	ω	$I_q(\omega)$	Mmean	W	$E(T)$	T_c	S
May	384	384	714.9	130.5	0.0009177	0.6349	0.3477	0.302	3.046	0.5	1614	0.3026	174	-10062	1500	-36.87
June	409	409	1282	1282	0.000914	0.5	0.5	0	1.886	0.5	3492	0	0	0	1500	-37.3
July	1661	1661	2452	0.0009234	0.8	0.7	0.0023	1.886	0.5	1774807	0	3492	0	0	1500	0
September	107	107	300.0	1435	0.0009053	0.8262	0.4148	0.607	4.022	0.5	246264	0.6074	1544	-392303	1500	-18.84
October	30	30	100.0	13.7	0.000917	0.6114	0.3853	0.603	3.04	0.5	26233	0.603	1435	-28	1500	-34.84
November	104	104	300.0	1435	0.0009053	0.8262	0.4148	0.607	4.022	0.5	246264	0.6074	1544	-392303	1500	-18.84
December	0	0	100	180.0	0.000904	0.8	0.7	0.0023	1.886	0.5	1620	0	0	0	1500	-36.09
January	0	0	20	20.0	0.000904	0.8	0.7	0.0023	1.886	0.5	1620	0	0	0	1500	-36.09
WE (<i>P. violaceum</i>)	$N_b \approx G \approx F \approx h$	NN	$u \approx a$	$T_b \approx b$	q	κ	κ'	$\theta(q)$	η_q	ω	$I_q(\omega)$	Mmean	W	$E(T)$	T_c	S
WE (<i>P. violaceum</i>)	$N_b \approx G \approx F \approx h$	NN	$u \approx a$	$T_b \approx b$	q	κ	κ'	$\theta(q)$	η_q	ω	$I_q(\omega)$	Mmean	W	$E(T)$	T_c	S
May	76	76	109	109	0.0009174	0.5	0.5	0	1.886	0.5	3492	0	0	0	1500	-37.3
June	124	124	714.9	130.5	0.0009177	0.6349	0.3477	0.302	3.046	0.5	1614	0.3026	174	-10062	1500	-36.87
July	1252	1252	1329	1329	0.0009151	0.5	0.5	0	1.886	0.5	3492	0	0	0	1500	-37.3
August	0	0	1561	1561	0.0009234	0.8	0.7	0.0023	1.886	0.5	1036001	0	20019	0	1500	0
September	0	0	1007	1007	0.00091	0.8074	0.4029	0.717	4.13	0.5	44052	0.4148	1435	-20280	1500	-24.81
October	0	0	1009	1009	0.000904	0.8262	0.4148	0.607	4.022	0.5	246264	0.6074	1544	-392303	1500	-18.84
November	0	0	101	101	0.0009053	0.8262	0.4148	0.607	4.022	0.5	246264	0.6074	1544	-392303	1500	-18.84
December	0	0	30	30.0	0.000904	0.8	0.7	0.0023	1.886	0.5	1620	0	0	0	1500	-36.09
January	0	0	301	301	0.001005	0.7456	0.4028	0.602	4.022	0.5	5206	0.6029	100	-26942	2090	-34.06
WW (population)	$N \approx G \approx F \approx h$	NN	$u \approx a$	$T_b \approx b$	q	κ	κ'	$\theta(q)$	η_q	ω	$I_q(\omega)$	Mmean	W	$E(T)$	T_c	S
WW (population)	$N \approx G \approx F \approx h$	NN	$u \approx a$	$T_b \approx b$	q	κ	κ'	$\theta(q)$	η_q	ω	$I_q(\omega)$	Mmean	W	$E(T)$	T_c	S
May	109	109	849.7	301.1	0.0009036	0.9921	0.3079	0.305	3.411	0.5	29397	0.3827	918	-14498	2090	-30.90
June	1666	1666	3000	1614	0.000914	0.5	0.5	0	1.886	0.5	3492	0	0	0	1500	-37.3
July	1430	1430	3123	1844	0.000943	0.8262	0.4148	0.607	4.022	0.5	246264	0.6074	1544	-392303	1500	-18.84
August	124	124	714.9	130.5	0.0009177	0.6349	0.3477	0.302	3.046	0.5	1614	0.3026	174	-10062	1500	-36.87
September	1017	1017	3029	692.7	0.001007	0.9793	0.4026	0.301	3.046	0.5	3888	0.3888	2090	-3024880	2090	-30.14
October	107	107	300.0	1435	0.0009053	0.8262	0.4148	0.607	4.022	0.5	246264	0.6074	1544	-392303	1500	-18.84
November	107	107	300.0	1435	0.0009053	0.8262	0.4148	0.607	4.022	0.5	246264	0.6074	1544	-392303	1500	-18.84
December	107	107	300.0	1435	0.0009053	0.8262	0.4148	0.607	4.022	0.5	246264	0.6074	1544	-392303	1500	-18.84
January	202	202	1240	800	0.001005	0.6926	0.3472	0.316	3.009	0.5	100953	0.3056	807	-20976	2090	-30.54
WW (<i>P. pallidum</i>)	$N_b \approx G \approx F \approx h$	NN	$u \approx a$	$T_b \approx b$	q	κ	κ'	$\theta(q)$	η_q	ω	$I_q(\omega)$	Mmean	W	$E(T)$	T_c	S
WW (<i>P. pallidum</i>)	$N_b \approx G \approx F \approx h$	NN	$u \approx a$	$T_b \approx b$	q	κ	κ'	$\theta(q)$	η_q	ω	$I_q(\omega)$	Mmean	W	$E(T)$	T_c	S
May	147	147	87.6	113.3	0.0008285	0.5	0.5	0	1.886	0.5	3492	0	0	0	1500	-37.3
June	147	147	130.7	111.3	0.0011226	0.5	0.5	0	1.886	0.5	3492	0	0	0	1500	-37.3
July	1535	1535	2818.3	614.5	0.001345	0.8077	0.4103	0.603	3.886	0.5	40013	0.603	1435	-240782	1500	-25.2
August	1530	1530	1310	1538	0.000903	0.8327	0.4053	0.802	4.055	0.5	460030	0.6054	1509	0	1500	0
September	809	809	2818.3	614.5	0.001345	0.8077	0.4103	0.603	3.886	0.5	40013	0.603	1435	-240782	1500	-25.2
October	309	309	708.8	308.7	0.001007	0.8237	0.405	0.8	3.886	0.5	170369	0.603	1435	-240782	1500	-25.2
November	309	309	708.8	308.7	0.001007	0.8237	0.405	0.8	3.886	0.5	170369	0.603	1435	-240782	1500	-25.2
December	91	91	300.0	1435	0.0009053	0.8262	0.4148	0.607	4.022	0.5	246264	0.6074	1544	-392303	1500	-18.84
January	0	0	91	91	0.001001	0.8	0.7	0.0023	1.886	0.5	1620	0	0	0	1500	-36.09
WW (<i>D. purpureum</i>)	$N_b \approx G \approx F \approx h$	NN	$u \approx a$	$T_b \approx b$	q	κ	κ'	$\theta(q)$	η_q	ω	$I_q(\omega)$	Mmean	W	$E(T)$	T_c	S
WW (<i>D. purpureum</i>)	$N_b \approx G \approx F \approx h$	NN	$u \approx a$	$T_b \approx b$	q	κ	κ'	$\theta(q)$	η_q	ω	$I_q(\omega)$	Mmean				

those of the individual averaged populations. As we see from considering the Weiss field $h = WM_{mean}$, M_{mean} is a solution of M . Note that W is an intensive parameter within a particular intra-active patch, as is the case for the definition of h . In a Weiss field, $T_s > W$ results in chaos and $T_s < W$ results in order, and thus W is likely to be the upper limit on T_s in the ordering (increasing) of a particular species. That is, a long-range order is only achieved when $T_s < W$, and if $T_s > W$, the output is disordered chaos [97]. $T_s = W$ is not applicable to this system, due to the mean-field approximation of the Weiss field. M_{mean} and W are listed in Table 4; note that some results reach the upper limit of $T_s \approx W$, indicating adaptation of a particular species denoted by W (Table 4, red characters). The value of W for the species is lower than that for the populations, indicating that the given species is easily able to dominate the overall population. If we set the long-range order parameter per individual to $p(T_s) = M_{mean}^2$ [97], empirically, $p(T_s) \leq 0.01$ seems to be an indicator of a stably adapted condition (Table 4). Comparing Table 1 with Table 4, except for $(\Re(s), \Im(s), m) = (2.056, 275.5, 2.994)$, they correspond to each other and are similar to a Bose-Einstein condensation [97]. The distinguishable individuals ought to behave as mutually exclusive fermions, but they could be treated as bosons, even when the number of fermions is known; when their number is large, they can be approximated as bosons. Bose-Einstein condensation is thus achieved, but only for the case in which $m \sim 0$.

Near the critical point $T_s \approx T_c$, M_{mean} is small and the susceptibility is approximately

$$\chi_T = U'(q_s) \propto |T_s - T_c|^{-1} \text{(Curie - Weiss law)}. \quad (70)$$

For the values of $U'(q_s)$ that approach infinity, in Figure 2, we graph q_s versus $U(q_s)$. Note that in both of the quadrats in the study region (Washidu East and Washidu West), the species we consider seem to have two phases for any given number of individuals; for small q_s , there is a species domination phase, and for large q_s , there is a chaotic phase without species differentiation. For the populations as a whole, we note that the Washidu East and Washidu West populations each have two phases for the total number of individuals; again, for small q_s there is a domination phase, and for large q_s there is a chaotic phase of individuals. From each quadrat, we averaged three temperatures that were close to $U'(q_s)$ as it approaches infinity, and we determined that the critical temperature is $T_c = 2090 \pm 50$ (95% confidence) for populations and 1500 ± 500 for species. This indicates that when $T_s > \sim 2090$,

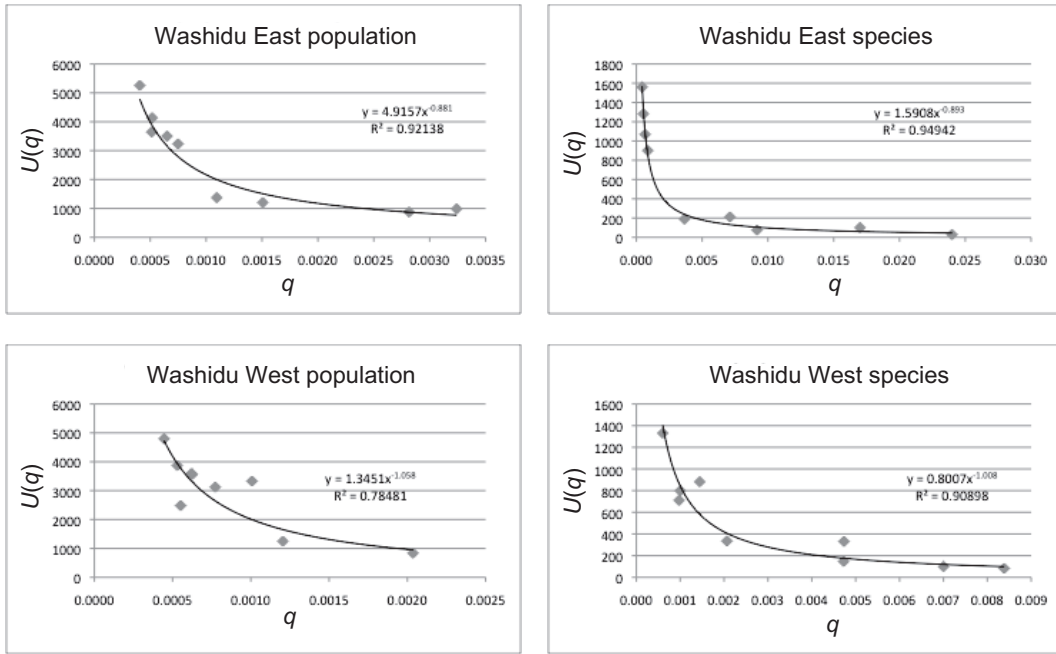


Figure 2: $U(q_s)$ for Dictyostelia fitted with power functions.

one population can uniquely dominate; when $T_s \sim 1500$ – 2090 , no population dominates, but a species can uniquely dominate. When $T_s < \sim 1500$, neither populations nor species dominate, and the system is chaotic, although the tendency of populations and species to increase still remains for $T_s < W$. These results are consistent with those obtained by considering the Weiss field, W . Note that the critical point T_c and Weiss field W are conceptually different: the former represents discontinuity of the overall phase, and the latter represents the conversion between ordered and disorders states [97]. Above the critical temperature for species, conversion between the dominating species phase and the increasing population phase is continuous, not discrete [97]. The domination phases and tendency to increase for each population or species are shown in Figure 3.

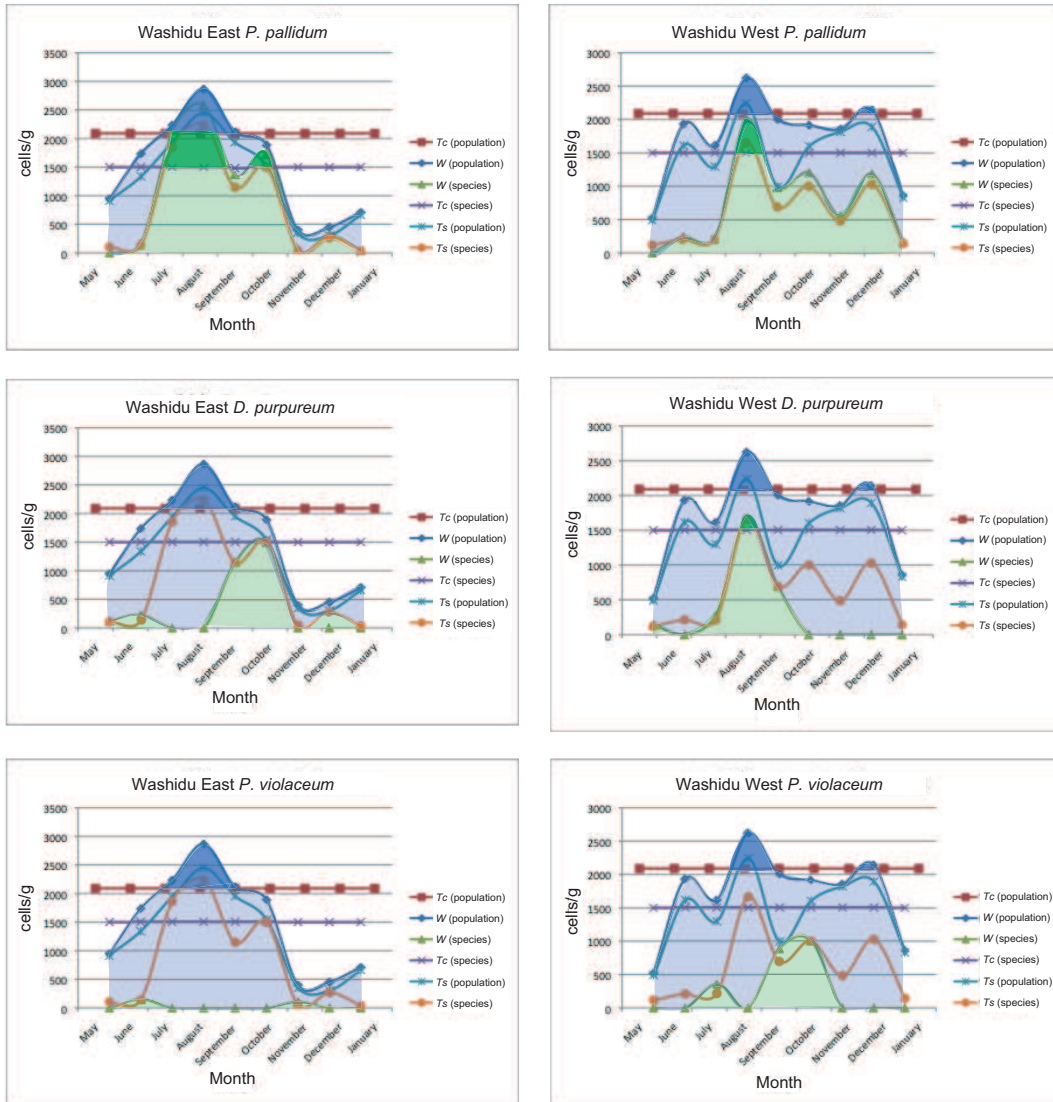


Figure 3: $W/T_c/T_s$ dynamics. *P. pallidum*: *Polysphondylium pallidum*; *D. purpureum*: *Dictyostelium purpureum*; *P. violaceum*: *Polysphondylium violaceum*. Dark blue shading indicates a phase in which the given population dominates; light blue indicates a phase in which a population is increasing; dark green indicates a particular species dominates; and light green indicates that a particular species is increasing. Populations include all species within the system, and are thus not restricted to the species labeled at the top of each figure.

Furthermore, $T_s < T_c$ increases the internal energy,

$$E(T_s) = -\bar{N}h \tanh(q_s h) \approx -\bar{N}q_s h^2, \quad (71)$$

when \bar{N} is N_k averaged over patches in populations or species. When $T_s > T_c$, $E = 0$, and when $T_s < T_c$, E is proportional to $T_c - T_s$. The specific heat $C_s (= \partial E / \partial T_s |_{h=0})$ is 0 at or above T_c , it is finite at or below the T_c , and it has a sudden increase at T_c . Usually, species have higher internal energy than do populations. The critical point can be determined by using data specific to a given species; note that there are several phases for population and species, including domination, increasing, and chaos.

3.9. Introducing large S , an order parameter

For the population space defined above and the volume of the system $V = 1$ for 1 gram of soil, we define S near the critical points as follows:

$$f\{S\} = f_0 + A'S^2 + B'S^4 - h'S, \quad (72)$$

where $f = F \approx G$ is the Hamiltonian; h' is the flow of the population from outside; and f_0 , A' , and B' are coefficients approximated by an expansion and assuming $B' > 0$ and $A' = A''(T_s - T_c)$, in which A'' is another approximated coefficient. At equilibrium,

$$\frac{\partial f}{\partial S} = 4B'S^3 + 2A''(T_s - T_c)S - h' = 0, \quad (73)$$

and the solution is the order parameter. When $h' = 0$, $S = 0$ is the only solution of $T_s > T_c$. An additional solution, $S \approx \pm(T_c - T_s)^{1/2}$, exists when $T_s < T_c$, with h' breaking the symmetry. The isothermal susceptibility is $\chi_T \approx |T_s - T_c|^{-1}$. When $T_s = T_c$, we have $S \approx h'^{1/3}$. When $C_0 = -T_s \partial^2 f_0 / \partial T_s^2$, we have the specific heat $C_s = C_0$ at $T_s > T_c$, $C_s = T_s A''^2 / 2B'$ at $T_s < T_c$, and a jump at $T_s = T_c$. The calculated values of S are listed in Table 4. The results indicate that there is a tendency towards order when a population or species dominates.

3.10. Application of the type IV Painlevé equation to an X^2 system

We will now discuss the development of time-related function t (time is actually t^2) in our system. Assume that X^2, XY, Y^2 (instead of X, Y ,

as modeling the selection of the interactions among X, Y ; that is, X^2, Y^2 correspond to N_X, N_Y and XY is a term of interaction) obey the Lotka-Volterra equations, which are equivalent to the type IV Painlevé equations:

$$\frac{dX^2}{dt} = X^2(XY - Y^2), \quad \frac{dXY}{dt} = -XY(X^2 + Y^2), \quad \frac{dY^2}{dt} = Y^2(XY - X^2). \quad (74)$$

The system represents the adaptive species situation discussed in the previous subsection and has the required symmetry. If the second equation is converted to $\frac{dXY}{dt} = XY(X^2 + Y^2)$, then the system becomes cooperative. To obtain \tilde{X} , simply divide the equation by $2X$. Now let us consider $N_P(t) = 1/X$. We apply the Verhulst logistic equation model proposed by [59]:

$$\frac{dN_P(t)}{dt} = N_P(t)(a_P(t) - b_P(t)N_P(t)). \quad (75)$$

Therefore, $a_P(t) = -XY/2$, $b_P(t) = -XY^2/2$, and if we set $c_P(t) = e^Y$,

$$N_P(t+1) = N_P(t)^{\frac{1}{1+b}} c_P(t)^{\frac{1}{b(1+b)}}, \quad (76)$$

and $t = b \arg D$ is properly selected. Note that a gauge function $h_t(t_t)$ will be $(\ln t_t^{-1})^{m_h - 1}$ where $t_t = e^{-\frac{1}{b}}$ and $m_h = \Re(s)$ [57]. From this, it is clear that the root of time is proportional to the temperature b of $N_k = a - b \ln k$ (not $b(t)$ in the above equation), and the inverse temperature is related to the root of generation time, which is the inverse of t . Next, consider an absolute zeta function

$$\zeta_{\mathbb{G}_m/F_1}(s) = \frac{s}{s-1} = \frac{s}{w}, \quad (77)$$

when $\mathbb{G}_m = GL(1)$. Note that s/w is the value of s for a particular group during the previous time step. Therefore, $\arg w = \arg D = 1/b$ (time and $\arg D$ are measured in opposite directions). If we consider $\mathbb{G} : \mathbb{H}/|\mathbb{H}| \times \mathbb{R} \times \mathbb{R}$ in terms of introducing $\mathfrak{S}(s)$ to explain adaptation/disadaptation of a species, there is a unique irreducible unitary representation $\rho_G : \mathbb{G} \rightarrow GL(W)$, besides an isomorphism, and for any $c_G \in \mathbb{H}/|\mathbb{H}|$,

$$\rho_G(c_G) = c_G \text{Id}_W \quad (78)$$

when Id_W is an identity mapping (Stone-von Neumann theorem; [93, 105, 106, 94]). This representation characterizes the system, which is still not possible at this moment.

Let us further expand this approach. Consider the Gauss equation with rational α, β, γ :

$$t(1-t)y'' + \{\gamma - (\alpha + \beta + 1)t\}y' - \alpha\beta y = 0. \quad (79)$$

If we select a quotient of two linearly independent solutions of the equation, $w_y(t) = y_1/y_2$, the Schwarz equation is

$$\left(\frac{w_y''}{w_y'}\right)' - \frac{1}{2}\left(\frac{w_y''}{w_y'}\right)^2 = \frac{1}{2}\left(\frac{1-\lambda^2}{t^2} + \frac{1-\mu^2}{(t-1)^2} + \frac{\lambda^2 + \mu^2 - \nu^2 - 1}{t(t-1)}\right) \quad (80)$$

when $\lambda^2 = (1-\gamma)^2$, $\mu^2 = (\gamma-\alpha-\beta)^2$, and $\nu^2 = (\alpha-\beta)^2$. Next, consider $y = D$. When $b \neq 0$, the branch points of w_y : $t = 0, 1, \infty$ are $\arg D = 0, 1/b, \infty$, respectively. Since $\arg D$ should be $\lambda\pi, \mu\pi, \nu\pi$, respectively, we obtain $\gamma = 1$ and $\gamma - \alpha - \beta = \pm 1/(b\pi)$. Therefore,

$$w_y' = \frac{y_1}{y_2} = \frac{\text{constance } t^{-\gamma}(t-1)^{\gamma-\alpha-\beta-1}}{y_2^2} = \frac{\text{constance } t^{-1}(t-1)^{\pm\frac{1}{b\pi}-1}}{y_2^2}, \quad (81)$$

and $y_1 = y_2 = D$ results in

$$D = \pm \sqrt{\frac{\text{constance}}{t(t-1)^{1\mp\frac{1}{b\pi}}}}. \quad (82)$$

Assuming t proceeds in the negative direction (because $D > 1$),

$$D_{t-1} = \sqrt{\frac{(t-1)^{\mp\frac{1}{b_t\pi}} \frac{t}{(t-2)^{1\mp\frac{1}{b_{t-1}\pi}}}}{D_t}} \quad (83)$$

when $t \neq 0, 1, \infty$ (double-signs correspond). Thus,

$$D = \left\{ (t-1)^{\mp\frac{1}{b_t\pi}} \frac{t}{(t-2)^{1\mp\frac{1}{b_{t-1}\pi}}} \right\}^{\frac{1}{2t}}. \quad (84)$$

For $t = 0, 1, \infty$, consider the Gauss hypergeometric function:

$$F_G(a_F, b_F, c_F; z_F) = \frac{\Gamma(c_F)}{\Gamma(a_F)\Gamma(c_F - a_F)} \int_0^1 t_F^{a_F-1} (1-t_F)^{c_F-a_F-1} (1-t_F z_F)^{-b_F} dt_F. \quad (85)$$

The solutions for $t = 0$ are

$$y_{1,0} = F_G(\alpha, \beta, \gamma; t) = \infty, \quad (86)$$

$$y_{2,0} = t^{1-\gamma} F_G(\alpha - \gamma + 1, \beta - \gamma + 1, 2 - \gamma; t) = \infty. \quad (87)$$

The solutions for $t = 1$ are

$$y_{1,1} = F_G(\alpha, \beta, \alpha + \beta - \gamma + 1; 1 - t) = \infty, \quad (88)$$

$$y_{2,1} = (1 - t)^{\gamma - \alpha - \beta} F_G(\gamma - \alpha, \gamma - \beta, \gamma - \alpha - \beta + 1; 1 - t) = \infty. \quad (89)$$

These solutions arise from the assumptions of our biological model. The actual converged values of D , including $t = 2$, should be validated either by observation or by calculation from other time points. The solutions for $t = \infty$ are

$$y_{1,\infty} = t^{-\alpha} F_G(\alpha, \alpha + 1 - \gamma, \alpha - \beta + 1; 1/t) = 0, \quad (90)$$

$$y_{2,\infty} = t^{-\beta} F_G(\beta, \beta + 1 - \gamma, \beta - \alpha + 1; 1/t) = \infty, \quad (91)$$

as expected. For the purposes of model validation, we neglect the values from populations because t is usually close to 1 or 2, indicating the values are not converging (chaos). Setting $b_t \sim b_{t-1}$ when $t \gg 1$, we examined 21 calculable values of species and omitted three values (October for Washidu West *D. purpureum*, $N = 0$; August for Washidu West *P. violaceum*, $N = 0$; and September for Washidu West *P. violaceum*, $\Re(s) = 0.32$, which is too small); the observed/expected D values are shown in Figure 4. A Student's t test indicated that our model was a good fit to the observations ($p = 0.809$). Pearson's χ^2 similarly indicated the extent of the match ($\chi^2 = 1.281$, $p = 1.000$).

For population-level dynamics, it is difficult to predict outputs directly because of the chaotic situation. However, we can introduce a newly defined $\Re(s)_l$ as follows. Consider a lemniscate function of

$$r^2 = 2a_l^2 \cos 2\theta, \arg D = r = \frac{1}{b}t, a_l = \frac{1}{b}. \quad (92)$$

We can set an almost confluent situation of individual population growth with $b \sim 1$ and $E(\Sigma N) \sim 1$. Since $\theta = \arg \arg D = 2\pi e^{\Re(s)_l}$,

$$\Re(s)_l = \ln \left\{ \frac{\arccos(\frac{1}{2}t^2)}{4\pi} \right\}. \quad (93)$$

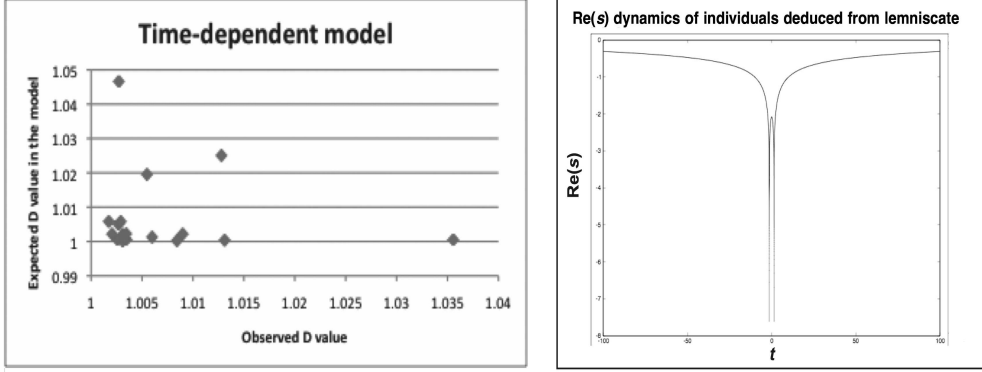


Figure 4: Plots of observed and expected D values in the time-dependent model, and individual $\Re(s)_t$ dynamics from the lemniscate.

The values among populations are likely to be negative and sometimes close to -3 . The trend is adaptive/disadaptive when the value is ~ -3 . From these calculations, we can estimate the overall trend of the growth/decline of a metapopulation; see the right panel in Figure 4.

3.11. Development of the model by web-based formalism

Here, we introduce an analogy to supersymmetry to further describe the time development of our model. This is Hodge-Kodaira decomposition for ϕ function:

$$I\phi^j(\Re(s)) = \bigoplus_{p_s+q_s=j} I\phi^{p_s,q_s}(\Re(s)), \quad (\overline{\phi^{p_s,q_s}(\Re(s))}) = \phi^{q_s,p_s}(\Re(s)) = \phi^{p_s,q_s}(-\Re(s)), \quad (94)$$

where $I : \phi \rightarrow v = \ln N_k / \ln \Im(s)$ for cohomology group as in [2].

First, consider Bochner's conjecture: for ϕ to be a characteristic function of the probability, the following three conditions are both necessary and sufficient: (I) $|\phi|/2$ is a positive constant; (II) $|\phi(\Re(s))|/2$ is continuous when $\Re(s) = 0$; (III) $|\phi(0)|/2 = 1$. Therefore, $\phi(-\Re(s)) = \overline{\phi(\Re(s))}$. Next, we consider the transactional interpretation of quantum physics [16], or Hodge-Kodaira decomposition to explain the time symmetry of our model. Based on this, we develop a supersymmetry matrix:

$$\frac{1}{2} \begin{pmatrix} \text{F4} : \phi(\Re(s)) & \text{F1} : \overline{\phi(-\Re(s))} \\ \text{F2} : -\phi(-\Re(s)) & \text{F3} : \phi(\Re(s)) \end{pmatrix},$$

where combinations of F4/F1 and F3/F2 are advanced/retarded waves and the determinant $\frac{1}{2}(F4F3-F1F2)$ is past-future. Here, $\phi(\Re(s))/\overline{\phi(-\Re(s))}$ is the absorber/observer, and $-\phi(-\Re(s))/\overline{\phi(\Re(s))}$ is the emitter/observant; note that $\overline{\phi(\Re(s))}$ is the past and $-\phi(-\Re(s))$ is the future. In a complex-based system, the $(-1+i)$ -adic system can be used to represent all complex numbers, whereas the $(1-i)$ -adic system cannot [50]. Moreover, when n is natural, only $-n \pm i$ can be used to represent all complex numbers. Thus, F1 of the observer represents the information of all possible futures, while the observed F4 cannot represent all possibilities; this results in an asymmetry between the past and future. Although all scenarios may have been part of the past, the future is restricted to a particular scenario. In the same way, F2 cannot represent all possibilities, but F3 can. This is the opposite of the relationship between the observant and observer.

To expand this interpretation, consider [advanced-retarded] waves as a realization of the future population, F4-F1 and F3-F2, in the $(\pm 1 \pm i)$ -adic system. F4-F1 represents a population increase, and F3-F2 represents a population decrease. Their geometric mean is $2\sqrt{(\cos \theta + i \sin \theta)(\cos \theta - i \sin \theta)} = 2$. Recall that bosons and fermions are orthogonal, based on the difference in their argument $\pi/2$, as in previous sections. The expected integral of this function is

$$\int_0^{\frac{\pi}{2}} \frac{d\theta}{2\sqrt{(\cos \theta + i \sin \theta)(\cos \theta - i \sin \theta)}} = \frac{\pi}{4}. \quad (95)$$

Remember that for an individual, the argument should be $\pi/4$, and an individual cannot represent the whole in the $(+1+i)$ -adic system. To represent the whole, it is necessary to use a three-dimensional $(-1+i)$ -adic system with an argument of $3\pi/4$, such as X^2, XY , and Y^2 . For example, consider

$$2 \int_{-1}^1 \sqrt{1-x^2} dx = 2 \int_{-1}^1 \sqrt{(1+i\sqrt{x})(1-i\sqrt{x})(1+i\sqrt{-x})(1-i\sqrt{-x})} dx = \pi. \quad (96)$$

The integral over population changes from -1 (decrease) to $+1$ (increase) of the geometric mean of probabilities of the potential in (*population increase probability*)² with past and future (correspond to $1+i\sqrt{\pm x}$) and (*population decrease probability*)² with past and future (correspond to $1-i\sqrt{\pm x}$) results in $\pi/2$. Therefore, the expected value of the concomitant increase/decrease of two interactants

is expected to be $\pi/2 (< 2)$. Similarly,

$$\int_{-1}^1 \frac{dx}{\sqrt{1-x^2}} dx = \int_{-1}^1 \frac{dx}{\sqrt{(1+i\sqrt{x})(1-i\sqrt{x})(1+i\sqrt{-x})(1-i\sqrt{-x})}} = \pi. \quad (97)$$

Therefore, the number of interacting dimensions (reciprocal of the expected probability) of the ± 1 fluctuation is close to three. Furthermore,

$$\int_{-\infty}^{+\infty} \frac{dx}{1+x^2} = \int_{-\infty}^{\infty} \frac{dx}{(1+ix)(1-ix)} = \pi. \quad (98)$$

Considering all the potentials of a particular wave function, the expected dimensions should be close to three. In other words, the dimensionality of the F3 potential is equal to that of the F4 potential $+ 2\pi x$.

The above system of matrices is obviously $SU(2)$. Since the system is also a Kähler manifold without $s = 1$, the four-dimensional Riemann manifold of the system becomes a Ricci-flat Kähler manifold/Calabi-Yau manifold [51]. The system also has Riemann curvature tensors with self-duality, since it is a two-dimensional Ising model [97]. Furthermore, it is assumed to be asymptotically locally flat, and therefore the ϕ space is an instanton. If we set \overline{W}_z , where a superpotential $W_z = \phi \frac{N_k+1}{N_k} (\Phi - e^{-iN\vartheta} \frac{\Phi^{N_k+1}}{N_k+1})$ for $\Phi = \phi i$, this is analogous to the ϕ - instanton equation described by [32]:

$$\left(\frac{\partial}{\partial x} + i\frac{\partial}{\partial \tau}\right)\Phi^I = \frac{i\phi}{2} g^{I\overline{J}} \frac{\partial \overline{W}_z}{\partial \overline{\Phi}^{\overline{J}}}, \quad (99)$$

where x is the genetic information, τ is time, $g^{I\overline{J}}$ is a metric tensor, and $\Re(\phi^{-1}W_z)$ and $\Im(\phi^{-1}W_z)$ are the Hamiltonian and the potential of the system, respectively. Assuming the unified neutral theory, Φ itself is a quantum critical point. This is because within the population system, it is assumed to be in equilibrium with the highest adaptation in the ordered state, and the lowest value of the critical temperature is $T_{qc} = 0$. Thus, each individual in the population has an equal role. With a vacuum weight $v_{ij} = v_i - v_j$, where $v_i = \phi \overline{W}_{zi}$, the worldline is parallel to v_{ij} . The vacuum configurations Φ_i and Φ_j exhibit a boundary for each critical point/state. When $e^{i\theta} \frac{W_{ji}}{|W_{ji}|} = \phi$, Φ_i is a boosted soliton of the stationary soliton Φ_j , and these define the edges of the webs [32].

3.12. Implications of the model as a nine-dimensional system

When $|N(p)|$ is 1 or 2/3, this suggests that the model described here has $\mathcal{N} = 2$ supersymmetry with three dimensions. In the previous subsection, we included supersymmetry, and in this subsection, we include three-dimensionality in the model. The equation that we need was presented in [41]; this is the original work, which contained a serious misprint; for corrections and details, see [42]:

$$(\Delta\Phi)^2 \approx \Lambda^{4/3}\Phi^{2/3}. \quad (100)$$

To apply this equation, we need an analogue to the speed of light and to the uncertainty principle. For the speed of light, recall that

$$\frac{\partial\mathfrak{R}(s)}{\partial t} = b\frac{1}{|D|}\frac{\partial|D|}{\partial t}. \quad (101)$$

This is analogous to Hubble's law for $H(t)$:

$$\frac{dD}{dt} = H(t)D, \quad (102)$$

with

$$\frac{\partial\mathfrak{R}(s)}{\partial t} = bH(t). \quad (103)$$

Note that $\max(dD/dt) = |D|^{E(\Sigma N)}$ for the observed system. The parameter analogous to the speed of light is therefore $|D|^{E(\Sigma N)}$. If we consider the time-dependent function D considered in the previous sections, then we have

$$H(t) = \frac{1}{D}\frac{dD}{dt} = \frac{t^2 - 4t + 2}{2t^2(t-1)(t-2)} - \frac{1}{2t^2}\ln\left[\{(t-1)^{\mp\frac{1}{b_t\pi}}\frac{t}{(t-2)^{1\mp\frac{1}{b_{t-1}\pi}}}\}\right]. \quad (104)$$

The uncertainty principle can be written as $\Delta D\Delta p_m \geq \hbar/2$, where $p_m = M_{mass}\dot{D}$. We can set $\hbar = 1$. If we set $M_{mass} = H(t)^{-1} = \phi \approx \text{constant}$ and $D = 1 + \Delta N_k$, then the uncertainty principle simplifies to $(\Delta\Delta N_k)^2 \geq 1$; obviously, this condition is fulfilled by the system by changing D . Since $|dD/dt| = |D|^{E(\Sigma N)}$ is only achieved when $\phi = 0$, the condition for the analogy to the photon is appropriate.

Now, let $|\Phi| = N_k/E(\Sigma N) \propto T_s$ in equilibrium. If G is an analogue of the gravitational constant, the Planck scale can be written as $\Lambda = \sqrt{\hbar G/|D|^{3E(\Sigma N)}}$.

When ϕ_i is the mass of the internal populations and ϕ_e is that from the external populations, we can set $V_p = GM_i M_e / D \approx \phi_i$. Note that $G = D / \phi_e = 1 / (\phi_e - \Delta\phi_e) \approx \text{constant}$ ($\phi / D = PD^{N_k-1} = \phi - \Delta\phi$), and $\Lambda^2 \approx \text{constant}$. Therefore $(\Delta\Phi)^3 \propto \Phi$, that is, Φ is the third power of its fluctuation, assuming $D^{E(\Sigma N)} = \text{constant}$. If we apply $\mathcal{N} = 2$ supersymmetry with the three-dimensional Ising model [9], then the kink is $\Delta = |N(p)| = 2/3$ and the superpotential is $\mathbf{W} = \Phi^3$. The dimensionality of the Ising model should be three. Next, we consider the Stefan-Boltzmann law. Since the entropy density is $s_d = 4U/3T_s \propto T_s^3$, there are nine dimensions in $s_d \propto \mathbf{W}$; this is similar to the case in superstring theory. Note that \mathbf{W} and s_d are in opposite directions. We can also set a three-dimensional fermionic Grassmann number, similar to what we did with string theory, if we assume a zero-sum patch game of the unified neutral theory and assume the fitness is w . The future predicted by the model is the Eisenstein series with $w_Q = 3$ [61]. Overall, based on the requirements from $\mathbf{W} = \Phi^3$ and $w_Q = 3$, w_Q should be 3 and $|N(p)| = 1$ should be in the interacting mode.

Additionally, according to [92], for a universe with constant ϵ , the scale factor $a(t)$ and the Hubble radius $H(t)^{-1}$ are related by the Friedmann equations with our modification of the $t \rightarrow t^2$ correspondence in $H(t)$ (that is, time emerges from a self-interaction of a particular potential $\mathfrak{S}(s)$):

$$a(t) \approx t^{2/\epsilon} \approx (H(t)^{-1})^{1/\epsilon}. \quad (105)$$

Let us set $\epsilon \equiv 3/2 * (1 + \varpi)$. In this system, $\varpi > 1$, $-1/3 < \varpi \leq 1$, and $\varpi \leq -1/3$ correspond to contraction, oscillation, and expansion of the universe. Since $\epsilon = 1/\Delta$, $|N(p)| = 1, 2/3$ show expansion/oscillation of the universe. Therefore, the former mode represents expansion, and it turns into the latter mode with oscillation, not with expansion.

4. Discussion

The small s value is similar to WAIC [108] in the following regards. WAIC is

$$W_n = T_n + \frac{\beta}{n} V_n, \quad (106)$$

where T_n is a training loss, V_n is a functional variance and β is an inverse temperature. If we use a covariance instead of V_n , $\Delta z_k \ln D_k$ becomes similar

to WAIC of k . Therefore, s is a derivative form of an information criterion of maximum likelihood estimation.

In our PzDom model, under the effects of entropy, the populations/species are assumed to fluctuate for $\mathfrak{R}(s) \sim 1$ or $\zeta = 0$. However, there is another solution. From the fractal theory results shown in Figure 1, $\mathfrak{R}(s) = 2$ is the border between population and species for Dictyostelia in the box dimension of the system. In the ecological data set of ruderal vegetation presented by [83], we can deduce that the data pertain to opportunistic species because in most areas $\mathfrak{R}(s) > 2$. On the other hand, marine interstitial meiofauna on sandy beaches and tropical rocky shore snails should be from populations, or at least from equilibrium species, because of $\mathfrak{R}(s) < 2$. As discussed above, adaptation can be defined as fitness that is sufficient to go beyond the fluctuations of harmonic neutrality and the border to this region is at $\mathfrak{R}(s) = 2$. From the data, we also observe that species with larger values of s/D have greater fitness. Since the world in which $\mathfrak{R}(s) > 1$ results in absolute convergence of ζ , the species world is not a chaotic world, but there is structure in the community that depends on adaptation and hysteresis. It is obvious that from the original Price equation, $\mathfrak{R}(s) > 1$ means $\text{Cov} > 0$ and thus such a species/population is on a course of diverging characteristics. When $0 < \mathfrak{R}(s) < 2$, it is chaotic characterized by $\langle \tilde{\mathcal{R}}_{A,\Omega}^{[k]}, \varphi \rangle$. It is also obvious that from the original Price equation, $\mathfrak{R}(s) < 1$ implies that $\text{Cov} < 0$, and the characteristics of the species/population are converging.

Although $\mathfrak{R}(s)$ may be continuous except that populations/species are adapted to the observed environments, each species has some discrete characteristic variables. These are required by the quantization of D by T , and they imply adaptation (resp. disadaptation) and a population/species burst (resp. collapse) in a particular environment. Because environmental variables are always continuous, genetic/epigenetic characteristics are responsible for the discreteness of D . That is, either a discrete genetic/epigenetic background or a biological hierarchy is rendering discrete characteristics at a higher scale and are demanded by T . The spectrum of the Selberg zeta-function also reveals the discrete nature of both populations and species, but the spectra of populations and species are based on prime closed geodesics and are not necessarily related to adaptation/disadaptation. This means that populations can behave in either discrete or pseudo-continuous and redundant ways. Therefore, prime numbers are related to adaptive species, and prime closed geodesics with high degeneracy are related to populations. Since the

number of primes is on the order of $T \ln T$ and that of closed geodesics is $e^{(d-1)T}/T$, the number of prime closed geodesics is much greater than the number of primes, and this is the observed relation between population and species. By analogue, it is predicted that eukaryotic species adaptations are well correlated with speciation, while prokaryotic discreteness is not easily distinguished from that of the whole population. This might be a candidate for a proof of the discreteness of phenotypes observed among living organisms in nature [79], and it may be important to test the $|N(p)|$ value to distinguish which hierarchical dynamics are observed in a given data set. It is possible that if the Mathieu group corresponds to a mock modular form, such as a Maass form, then the dimensionality of the system can be calculated by using the Eisenstein series (for M_{24} ; e.g., [26]). Assuming that the K3 surface (s with an interaction) is a holomorphic symplectic symmetry group, it is a subgroup of the group M_{24} [69]. Now consider an oscillating part of an Eisenstein series: $e^{2\pi i n \Re(s)}$. First, consider a $(1+i)$ -adic system. Since $m\pi/4 = 2\pi n \Re(s)$, m should be a multiple of 8 if $\Re(s)$ is quantized as a Bose-Einstein condensate, as described in the Results. In contrast, a $(-1+i)$ -adic system results in $3m\pi/4 = 2\pi n \Re(s)$, and $3m$ should be a multiple of 24 as a Bose-Einstein condensate. A nontypical quantization with $m \sim 3$ thus might presumably represent a population burst/collapse not in equilibrium. When the system results from the interaction between two subsystems, these can be decomposed to four and twelve, respectively. For any observed state, having four dimensions is sufficient. However, this cannot represent every possibility. Twelve dimensions (with fluctuations) are needed to represent all possible unobserved states. In other words, classically, if we use Liouville's equations, $\partial\bar{\partial}\phi = 2\pi\mu_\phi b_\phi e^{2b_\phi\phi}$, $P^2 = 2\pi\mu_\phi b_\phi$, and $D = e^{b_\phi}$, the Weil-Petersson metric becomes $ds_\phi^2 = e^{2b_\phi\phi} dk d\bar{k} = \text{constant}$ (e.g., [25] with negative Ricci curvature. The uniformization theorem states that any Teichmüller space has uniquely defined solutions [74, 47, 75, 76, 52, 53, 54]. This case is prominent especially in genus number 3 on a closed Riemann surface with twelve real dimensions, as observed in Selberg zeta analysis. When the quantum dilogarithm function is e_b , the ideal tetrahedron is $\psi(Z_\psi) = e_b(Z_\psi/2\pi b_\phi + iQ_\psi/2)$ when $qa = \infty, qb = 1$, and $Z_\psi = \ln k$ (e.g., [99]); this represents three dimensions plus time with three-dimensional fluctuations (the fluctuations are from other than the dimension of interest). In this way, an expansion of the PzDom model to a time-developing system should have twelve dimensions. To support this idea, the (a, b, k) system could be $SO(3)$, and Vogel's parameters for a simple Lie algebra g are $\alpha = -2, \beta = 4, \gamma = -1$, and

$t = h^\vee = 1$ [67]. If we set a half sum of positive roots $\rho = 1$ as two interacting positive roots of 1, the Freudenthal-de Vries strange formula becomes $12\rho^2 = h^\vee \dim g = \dim g = 12$ (also see [67]), based on the relation between the interaction of the objects in ρ and time development in dimension 12. More simply, consider $w_k = s - 1 = -1$ when the natural boundary is $s = 0$. Then, $\psi = 1/k^{w_k} |\zeta(w_k)| = 12k$ and in the top-ranking population/species, the number of degrees of freedom for the fitness at the natural boundary should be 12. Finally, using Stirling's approximation, $\frac{\sqrt{2\pi}}{e} (1 + \frac{1}{12}) \approx 1$. This means that the ratio between the number of expected interactions when n is a significantly large number plus another interaction added to the system, and the number of expected interactions in the k th population/species plus another interaction added to the system, is close to $\sqrt{2\pi}$, which is the geometric mean of the number of interactions in two four-dimensional systems (deduced from the analysis presented above). This closely matches the four-dimensional system observed with the addition of interactive constituents, which is accomplished by replacing each system dimension with three other dimensions, which means $4 \times 3 = 12$ dimensions, as described.

Note that if $\Re(s - 1) \sim 1/2$, these are observations not in a structured species world but in a chaotic speciation world. If $\Re(s) > 2$, we observe the phenomena of a structured species world. It is also notable that for $\Re(s) = 2$ exactly, extremely complicated harmonic functions are generated by the boundary A of the Mandelbrot set and we still do not know whether it is Minkowski nondegenerate or degenerate mathematically [57].

When $\Re(s) - 1 > 0$, either the cooperative situation $q_b > 0$ with $\Re(s) < 2$ holds or $q_b = 0$ with $\Re(s) > 2$ without any interpopulational interaction seems to be achieved. Thus, the status of the $\Re(s)$ world is roughly separated into three cases: (i) chaotic: $0 < \Re(s) < 1$ with mutual exclusion; (ii) ordered: $1 < \Re(s) \leq 2$ with cooperation/speciation; and (iii) most adaptively ordered: $\Re(s) > 2$ with stability and no interaction (oscillating “nirvāṇa” state). According to Fermat's last theorem, the noninteracting mode of subpopulations with $q_b = 0$ is only achieved when $X^n + Y^n = Z^n$ with $n \leq 2$. It is predicted that there is a possible noninteracting mode in which only a second-order nirvāṇa state is continuously observed. Note that the nirvāṇa state is regarded as the state of the most dominant species, and it is for a particular set of species at a particular time; it is not regarded as a fixed state for any particular species. It is also notable that when the environment is stable, the nirvāṇa state is also stable. However, when the environment changes significantly, species from the previous nirvāṇa state will fall into a

chaotic state, rendering interactions involving competition, cooperation, and starvation-induced sexual reproduction with others. Therefore, outside of a nirvāṇa state, a species must interact with other species. Furthermore, co-evolving communities in different niches cannot be described by this model, and this is a limitation of our study. It is notable that for a given niche, a noninteracting nirvāṇa state is the one most likely to be dominated by a species. Consider now the Euler-Mascheroni constant:

$$\lim_{s \rightarrow 1} \left(\zeta(s) - \frac{1}{s-1} \right) = \gamma = 0.577\dots \quad (107)$$

When $k = 1$, $|\zeta(s)| = E(\Sigma N)/N_1$, and in a population, it is 0.5. Therefore, $w < 0$, and in the long run, the population decreases. In a species, when $N_1 \ll E(\Sigma N)$ in a speciation phase, $w > 0$. Even when $N_1 \approx E(\Sigma N)$, $w > 0$, and investing in a higher-order hierarchy of species from a populational hierarchy escapes the limit of the decreasing trend in mere populations. These species are overall adapted. The discussion here is summarized in Figure 5.

It is expected that in the nirvāṇa state, mutual exclusion of genetic information from different species is achieved via reproductive isolation mechanisms based on uniparental chromosome elimination [4, 31, 62].

Interestingly, [22] suggests that the scaling exponents are 2/3 for those that refer to the ratios of the fractional changes in metabolic rates to a change in body size among opportunistic species, such as annual plants and small animals (see also [111]), but for equilibrium species, they are unity for perennial plants and 3/4 for large animals. These values are similar to the values found for $|N(p)|$ in our model, though in this model, it is assumed that Euclidean surface area rules entail a unique minimal scaling exponent related to energy transduction localized in biomembranes. In our model, the objects are not metabolites related to biomembranes, and the assumption is not required; however, it is still possible for both models to produce metabolites with the same value. Furthermore, we showed that $a(t) \approx (M_{mass})^{|N(p)|}$. It might be interesting to survey the $|N(p)| = 3/4$ case, although we note that this is considered doubtful by [24], or to extend our study from Dictyostelium populations/species to lower-order hierarchies, such as individual/organic/tissue/cellular/organelar/molecular metabolisms. Hubble's law could be a common point from which to understand the background logic of different hierarchies.

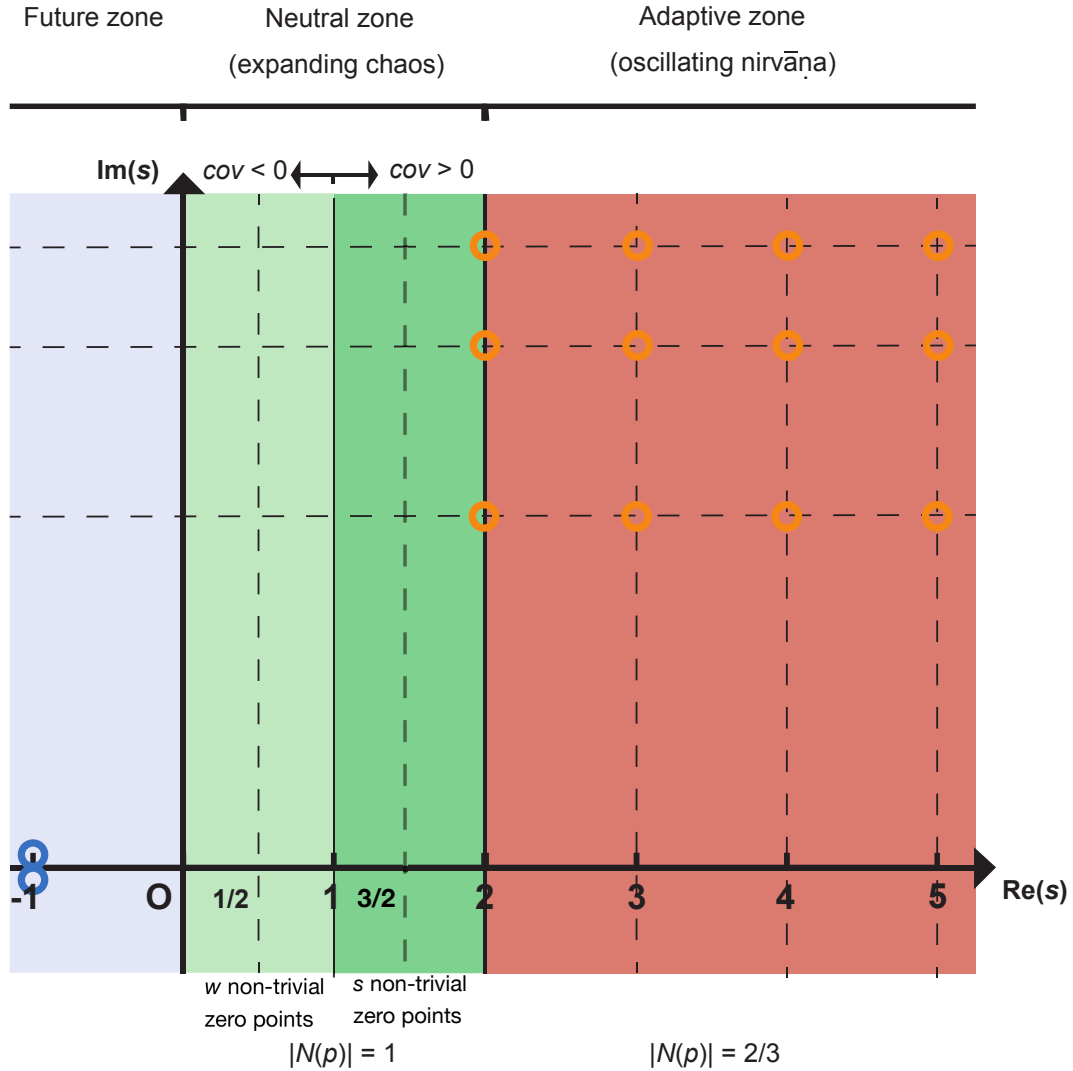


Figure 5: Visualization of an upper half-plane \mathbb{H} in the PzDom model. Nontrivial zeros of the Riemann ζ function, which represent a population burst/collapse, are assumed to be at the points where the $\Re(s-1) = 1/2$ axis intersects the horizontal broken lines (note that the scales of the horizontal and vertical axes differ). Orange circles represent adapted stages as species. The blue area represents a future stage with $[V_p = -\phi, \Re(s-1) \approx -1/(3\phi)$ and $\Im(s-1) \approx e^{-1/(3\phi)}$] [61]; converged states are indicated by blue circles. Note that $\Re(s)$ values with non-prime integers are theoretically unstable and are not observed empirically. $\Re(s) = 4$ is still remarked as orange circles for ramifications, however.

The output of the developed system is unpredictable when $T_s < T_c$; this is because the infinite volume limit of the system is not unique [97]. This might be the case for the simulated sympatric “speciation” presented by [18].

If there are two subgroups in a populations/species with frequency X/Y , then $w = w_0 + BY - CX$ when w_0 is the fitness without benefit from interactions, B is the benefit of X from Y , and C is the cost to X from the interaction. Since $|D|^{E(\Sigma N)}$ is the most promising virtual benefit from non-interacting individuals, w_0 and $\Re(s) - 1$ describe the overall fitness resulting from the interaction. $\Re(s) > 1$ thus results in a cooperative world of higher fitness accompanied by speciation, and $0 < \Re(s) < 1$ results in a competitive world with a population burst/collapse with discrete characteristics. Ordered symbiosis might be involved in $\Re(s) > 1$, and chaotic mutual exclusion might be involved in $0 < \Re(s) < 1$. This is also supported by the analysis of geodesics. When the s value is in the condition of $\Re(s) - 1 < 0$ for a significantly long duration that is not observed in [1], it is possible for $q_b < 0$ and the system is under highly competitive situation. For example, $|N(p)| = 1/3$ with a contracting universe. Note that q_b is the coefficient of XY in [118], and the populations/species is harmed by competition. This case is similar to the Chern-Simons action S_{CS} [115]:

$$S_{CS} = \frac{k_{CS}}{4\pi} \int_M \text{tr}(A \wedge dA + \frac{2}{3}A \wedge A \wedge A), \quad (108)$$

where k_{CS} is the integer level of the theory with a field strength of zero at all boundaries. A can represent X^2, XY , or Y^2 vectors, and the weight of the first term in the trace should be 0 in adaptive situations when X and Y are dependent. It should be $+1/3$ in cooperative situations and $-1/3$ in competitive situations. Chern-Simons theory thus describes the action in the PzDom model, and the time derivative of the action is the Lagrangian of the system. Since the Lagrangian is $T_s \ln k$, when $k = \text{constant}$, $dS_{CS}/dt \cdot dT_s = T_s \ln k dT_s$, and $dS_{CS} = \frac{\ln k}{2 \arg D} t^2$. Therefore, when $\arg D = \text{constant}$, $\int \int dS_{CS} dt = \frac{\ln k}{6 \arg D} t^3 = \frac{(\arg D)^2}{6} \ln k T_s^3$, and if $\arg D = \pi$, $\int \int dS_{CS} dt = \zeta(2) \ln k T_s^3 \propto s_d = \frac{4}{3} a_b T_s^3$ when $U = a_b T^4$ in black-body radiation; note that populations/species tend to pass this boundary. Thus, s_d is the volume of a non-Euclidean sphere with radius T_s when $a_b = C_c/d_c$, where C_c is the circumference and d_c is the diameter. Also note that $1/\zeta(2)$ is the probability that two randomly selected integers are disjoint. That is, $\ln k T_s^3$ is the expected interaction scale of $\int \int dS_{CS} dt$, which is T_s^3 multiplied by the relative entropy.

There is another way of setting the Lagrangian on a boson:

$$L = i\bar{\psi}\dot{\psi} - \epsilon\bar{\psi}\psi = |D|^2(i \ln |\dot{D}| - \epsilon). \quad (109)$$

If $\epsilon \rightarrow 0$, $T_s \rightarrow |D|^2$ and $|\dot{D}| \rightarrow k$, which simplifies the calculation. If we consider a sum of relative entropies $\sum \ln k$, then $\ln k! \approx \ln(\sqrt{2\pi k}(\frac{k}{e})^k) = \frac{1}{2} \ln(2\pi k) + k \ln(\frac{k}{e})$ when k is large. The partial time-differential of $\sum \ln k$ is approximately:

$$\frac{1}{2} \frac{1}{k} \frac{\partial k}{\partial t} + (\ln k) \frac{\partial k}{\partial t} = \left(\frac{1}{2|\dot{D}|} + \ln |\dot{D}| \right) |\ddot{D}|. \quad (110)$$

The Hamiltonian H_H utilizes a reflectionless potential and from discrete quantum mechanics, pure imaginary shifts [71]:

$$\lim_{\gamma \rightarrow 0} \gamma^{-2} H_H = p_m^2 - \frac{h_H(h_H + 1)}{\cosh^2 \mathfrak{S}(s)/b}, \quad (111)$$

where $h_H = -s$. Note that $i\mathfrak{S}(s)/b = i\pi/2(\text{mod } i\pi)$ has regular singularities.

Interestingly, if we set a p -adic field \mathbb{F} of p other than 2 or 3, then the necessary and sufficient condition for root 3 to exist in \mathbb{F} is that $p \equiv 1$ or $11 \pmod{12}$. Therefore, if we stick to three dimensions comprising the interactions of identical constituents, then $p \equiv 1$ or $11 \pmod{12}$ should be satisfied. This demonstrates the symmetry of the following equations. Note that the following equation was considered by Srinivasa Ramanujan (1916?) in an unpublished manuscript:

$$F(z) = q \prod_{n=1}^{\infty} (1 - q^n)^2 (1 - q^{11n})^2 = \sum_{n=1}^{\infty} c(n) q^n. \quad (112)$$

He proposed

$$L(s, F) = (1 - c(11)11^{-s})^{-1} \times \prod_{p \neq 11} (1 - c(p)p^{-s} + p^{1-2s})^{-1}, \quad (113)$$

and later, [27] proved that when $E : y^2 + y = x^3 - x^2$, $L(s, E) = L(s, F)$. It is well known that

$$\Delta(z) = q \prod_{n=1}^{\infty} (1 - q^n)^{24} = \sum_{n=1}^{\infty} \tau(n) q^n, \quad (114)$$

$$L(s, \Delta) = \prod_{p:\text{prime}} (1 - \tau(p)p^{-s} + p^{11-2s})^{-1}, \quad (115)$$

and (F, Δ) corresponds to $(1, 11)$ dimensions of the term p . Please note that both $F(z)$ and $\Delta(z)$ represent the interaction of two identical decompositions of 12 dimensions, multiplied by q_R . Note that $E : y^2 + y = x^3 - x^2$ implies $y(y + 1) = x^2(x - 1)$, and if the time of a phenomenon proceeds from x to $x - 1$, the interaction decreases from interacting x^2 to noninteracting decreased $(x - 1)$. However, mod 4 of the equation represents y as both zero and as a three-dimensional projection of the system. The solutions of the equation should be $(0, 0), (0, 3), (1, 0), (1, 3)$. Note that $y = 3$ means that the left-hand side of the equation should be $3 \times 4 = 12$ weights. This explains the time asymmetry of the system.

To expand this discussion, consider an icosahedron and quintic equation, as in [48]. Note that a dihedral group is a representation of two complex conjugates. An icosahedron is composed of six conjugate $n = 5$ dihedral groups and ten conjugate $n = 3$ dihedral groups. The quintic dimensions include three physical space dimensions, one time dimension, and a one-dimensional interaction axis. For $n = 5$, the dihedral groups can be interpreted as these quintic-dimensional functions, and the six conjugates come from the two interacting functions, each of three-dimensional fluctuations. For $n = 3$, the dihedral groups can be interpreted as the three-dimensional fluctuations, and the ten conjugates are the two interacting functions, each of quintic-dimensional functions. Fifteen cross lines correspond to fifteen four-groups (two conjugates), which are the four different types ($SU(2)$) of interactions between a dimension and a three-dimensional space minus one. The system of 16 weights is the first case in which the symmetry can be completely broken, which is required for the development of the system [96, 116].

To expand the interpretation in Figure 5, consider the ϕ plane with a small s value on four-groups (three physical space dimensions + one time dimension). For the physical dimensions xyz , we can set ϕ and a real parameter ρ_P with a positive constant a and

$$\begin{cases} x = (a - \rho_P \sin \frac{1}{2} \arg \phi) \cos \arg \phi, \\ y = (a - \rho_P \sin \frac{1}{2} \arg \phi) \sin \arg \phi, \\ z = \rho_P \cos \frac{1}{2} \arg \phi. \end{cases} \quad (116)$$

A Paddelbewegung-like motion [110] follows $\rho'_P = (-1)^{n_\phi} \rho_P$, $\phi' = \phi + 2n_\phi \pi i$, where $n_\phi \sim N(T)$ and $2n_\phi \pi \sim \Im(s)$. For a torus, consider a radius r and

a distance to a point from the center R . Addition of a real parameter σ_P would lead to

$$\begin{cases} x = (R + r \cos \sigma_P) \cos \arg \phi, \\ y = (R + r \cos \sigma_P) \sin \arg \phi, \\ z = r \sin \sigma_P. \end{cases} \quad (117)$$

If we consider ϕ, σ_P as functions of t , $\frac{d\phi}{dt}$ & $\frac{d\sigma_P}{dt}$ as continuous, and $(\frac{d\phi}{dt})^2 + (\frac{d\sigma_P}{dt})^2 \neq 0$, the area of the surface $A_{\phi\sigma}$ would be

$$\left(\frac{dA_{\phi\sigma_P}}{dt}\right)^2 = (R + r \cos \sigma_P)^2 \left(\frac{d\phi}{dt}\right)^2 + r^2 \left(\frac{d\sigma_P}{dt}\right)^2, \quad (118)$$

ψ would be

$$\psi = \int_0^{\sigma_P} \frac{d\sigma_P}{\frac{R}{r} + \cos \sigma_P}, \quad (119)$$

and $dA_{\phi\sigma_P}^2 = (R + r \cos \sigma_P)^2 (d\phi^2 + d\psi^2)$. A point of a four group (ϕ, ψ) can be described as a translation group:

$$\begin{cases} \phi' = \phi + 2n_\phi\pi i \sim \phi + \Im(s)i, \\ \psi' = \psi + \frac{2\pi r}{\sqrt{R^2 - r^2}} n_\psi \sim \psi + \frac{2\pi}{2\pi} n_\psi \sim \psi + n_\psi, \end{cases} \quad (120)$$

where $\sin \theta_\psi = \frac{r}{R}$ as $\tan \theta_\psi = \frac{n_\phi}{T} \sim \frac{1}{2\pi}$ ($\tan \theta_\psi$ is a T -normalized quantized number n_ϕ). Thus, s and w approximately localize at and jump among positions of integer when $\Re(s) > 2$, as in orange circles of Figure 5.

In this study, we present new metrics T_c , W , and S for distinguishing between populations and species, based simply on knowledge of the total number of individuals. We thus demonstrated spontaneous symmetry breaking of a biological system. S describes the extent of ordering based on domination. The metrics presented here can also successfully evaluate the critical point T_c and the Weiss field W . They can distinguish between different ordering states, such as a random distribution, a dominant species, or a population; their potential phase transitions; and adaptations ($T_s \approx W$). The $T_s \approx W$ case represents a biological application of Bose-Einstein condensation to population dynamics [97]. The theory of similar condensation phenomena was described by [49]; besides the case in that paper, we are able to describe quantization with a case that is not a typical Bose-Einstein condensation. This is shown in Figure 3. The phase separation depends on the levels of biological hierarchies, such as a population and a species, and we can evaluate the adaptive structures allowed during the evolution in each phase: for

a population-dominant phase, a single population could dominate a community; for a species-dominant phase, not a population but a sum of a given species in a community could dominate. The increasing phases correspond to the introduction of the next domination phase. Additionally, we cannot be sure of the output of a chaotic phase. When the relative information entropy is maximized with absolute randomness or chaos, there is no order. On the other hand, when the relative information entropy is minimized with a uniform distribution, there is no pattern.

The model also shows that some highly adapted species are more stable than others. Furthermore, the zero points of the Riemann zeta function correspond to the adaptive species and also to prime numbers. The entropy $\ln k$, which was introduced in this manuscript, can be approximated by $\pi(k)/k \approx 1/\ln k$, where $\pi(k)$ is the prime counting function. The decrease in the prime number density along with the growth of entropy means that the tendency to decrease is only broken when higher-order hierarchies exist. Thus, for these organisms, higher-order hierarchies may serve as investments in adaptive ordering structures.

Now, let us consider biological hierarchies resulting from genes, cells, multicellular individuals, populations, and species. For genes and cells, if we restrict the surrounding environments to a small scale, such as cells or individuals, the copy numbers of genes and cells are nearly static, and they are no longer adaptive. Thus, $T_s \sim 0$ for these cases. The individuals surrounded by populations or the populations themselves are chaotic when $T_s \neq 0$. Our data suggest that the species level is more adaptive than are the lower-order hierarchies. For example, in Figure 3, dark blue shading indicates a population dominant phase for species dynamics as a whole, because in this regard, the entire population can be considered to be a species world; light blue, dark green, and light green indicate phases of populational chaos. We thus conclude that reproductive scales are chaotic, and to achieve adaptation, we need higher-order hierarchies. Lower-order hierarchies have the most adaptive situations, and we must extend observation from lower to higher environmental scales, such as species, communities, or ecosystems, to detect the selection pressures on genes or cells.

5. Conclusions

We have successfully applied the Price equation, the $R = T$ theorem, and Weil's explicit formula to an ecological model, which we refer to as the PzDom model, and which is based on a new topological parameter, small s . Species could be defined as a p -Sylow subgroup of a community in the single niche. The border between adaptive species and chaotic populations/species was found to be $\Re(s) = 2$ (also proven by fractal theory), and the values of the norm of prime closed geodesics are $|N(p)| = 2/3$ and $|N(p)| = 1$, respectively. Note that mod 4 of p reveals the adaptive/disadaptive situations and the Bose-Einstein condensates. The future adaptation/disadaptation of individuals is partially predictable by the Hurwitz zeta function, and we also found a time-dependent fitness function. Furthermore, we showed that it is a natural consequence of species adaptations, when considered as primes, or population conversions, when considered as geodesics, to observe a phenotypic discontinuity when maximizing information entropy. The model is able to prove the existence of biological phases of populations and species. The phases can be used to distinguish and predict different types of population and species, based on the population/species dynamics/distribution. This provides a ground map for future studies to increase our understanding of the nature of hierarchical systems.

Acknowledgements

I am grateful for the financial support from Tokushima University and Kyoto University, and I thank all the reviewers and colleagues who have provided me with useful comments and suggestions.

References

References

- [1] S. Adachi, Eastern Japanese *Dictyostelia* species adapt while populations exhibit neutrality, *Evol. Biol.* 42 (2015) 210–222. <https://doi.org/10.1007/s11692-015-9312-0>.
- [2] S. Adachi, Rigid geometry solves “curse of dimensionality” effects in clustering methods: an application to omics data, *PLOS ONE* 12 (2017) e0179180. <https://doi.org/10.1371/journal.pone.0179180>.
- [3] L. Arnold, V. Matthias, L. Demetrius, Evolutionary formalism for products of positive random matrices, *Ann. Appl. Probab.* 4 (1994) 859–901. <http://dx.doi.org/10.1214/aoap/1177004975>.
- [4] G.S. Bains, H.W. Howard, Haploid plants of *Solanum demissum*, *Nature* 166 (1950) 795. <https://doi.org/10.1038/166795a0>.
- [5] J.R. Banavar, A. Maritan, I. Volkov, Applications of the principle of maximum entropy: from physics to ecology, *J. Phys.: Condens. Matter* 22 (2010) 063101. <https://doi.org/10.1088/0953-8984/22/6/063101>.
- [6] M. Barluenga, K.N. Stölting, W. Salzburger, M. Muschick, A. Meyer, Sympatric speciation in Nicaraguan crater lake cichlid fish, *Nature* 439 (2006) 719–723. <https://doi.org/10.1038/nature04325>.
- [7] G. Bianconi, A.L. Barbási, Bose-Einstein condensation in complex networks, *Phys. Rev. Lett.* 86 (2011) 5632–5635. <https://doi.org/10.1103/PhysRevLett.86.5632>.
- [8] G. Bianconi, L. Ferretti, S. Franz, Non-neutral theory of biodiversity, *EPL* 87 (2009) 28001. <https://doi.org/10.1209/0295-5075/87/28001>.
- [9] N. Bobev, S. El-Showk, D. Mazác, M.F. Paulos, Bootstrapping the three-dimensional supersymmetric Ising model, *Phys. Rev. Lett.* 115 (2015) 051601. <https://doi.org/10.1103/PhysRevLett.115.051601>.
- [10] A. Bošković, O.J. Rando, Transgenerational epigenetic inheritance, *Ann. Rev. Genet.* 52 (2018) 21–41. <https://doi.org/10.1146/annurev-genet-120417-031404>.

- [11] T. Bridgeland, Flops and derived categories, *Invent. Math.* 147 (2002) 613–632. <https://doi.org/10.1007/s002220100185>.
- [12] E. Cahen, Sur la fonction $\zeta(s)$ de Riemann et sur des fonctions analogues, *Ann. Sci. Éc. Norm. Supér.* 3^e 11 (1894) 75–164. <https://doi.org/10.24033/asens.401>.
- [13] J.A. Capitán, J.A. Cuesta, J. Bascompte, Statistical mechanics of ecosystem assembly, *Phys. Rev. Lett.* 103 (2009) 168101. <https://doi.org/10.1103/PhysRevLett.103.168101>.
- [14] J. Chave, Neutral theory and community ecology, *Ecol. Lett.* 7 (2004) 241–253. <https://doi.org/10.1111/j.1461-0248.2003.00566.x>.
- [15] J.A. Coyne, H.A. Orr, *Speciation*, Sinauer Associates, Inc., Sunderland, 2004.
- [16] J. G. Cramer, The transactional interpretation of quantum mechanics, *Rev. Mod. Phys.* 58 (1986) 647–687. <https://doi.org/10.1103/RevModPhys.58.647>.
- [17] C. Darwin, *On the Origin of Species*, J. Murray, London, 1859.
- [18] M.A.M. de Aguiar, M. Baranger, E.M. Baptestini, L. Kaufman, Y. Bar-Yam, Global patterns of speciation and diversity, *Nature* 460 (2009) 384–387. <https://doi.org/10.1038/nature08168>.
- [19] A. Deitmar, The Selberg trace formula and the Ruelle zeta function for compact hyperbolics, *Abh. Math. Sem. Univ. Hamburg* 59 (1989) 101–106. <https://doi.org/10.1007/BF02942321>.
- [20] J.-B. de Lamarck, *Philosophie Zoologique*, vol. 1, Museum d’Histoire Naturelle, Paris, 1809.
- [21] A. Denjoy, L’Hypothèse de Riemann sur la distribution des zéros de $\zeta(s)$, reliée à la théorie des probabilités, *C. R. Acad. Sci. Paris* 192 (1931) 656–658.
- [22] L. Demetrius, The origin of allometric scaling laws in biology, *J. Theor. Biol.* 243 (2006) 455–467. <https://doi.org/10.1016/j.jtbi.2006.05.031>.

- [23] R.C. Dewar, A. Porté, Statistical mechanics unifies different ecological patterns, *J. Theor. Biol.* 251 (2008) 389–403. <https://doi.org/10.1016/j.jtbi.2007.12.007>.
- [24] P.S. Dodds, D.H. Rothman, J.S. Weitz, Re-examination of the “3/4-law” of metabolism, *J. Theor. Biol.* 209 (2001) 9–27. <https://doi.org/10.1006/jtbi.2000.2238>.
- [25] B.A. Dubrovin, S.P. Novikov, A. Fomenko, *Modern Geometry-Methods and Applications, part I, The Geometry of Surfaces, Transformation Groups, and Fields*, Graduate Studies in Mathematics 93, 2nd ed., Springer-Verlag, Berlin-Heidelberg-New York, 1992, p. 118.
- [26] T. Eguchi, H. Ooguri, Y. Tachikawa, Notes on the K3 Surface and the Mathieu group M_{24} , *Exper. Math.* 20 (2011) 91–96. <https://doi.org/10.1080/10586458.2011.544585>.
- [27] M. Eichler, Quaternäre quadratische Formen und die Riemannsche Vermutung für die Kongruenzzetafunktion, *Arch. Math.* V 1954 (1954) 355–366. <https://doi.org/10.1007/BF01898377>.
- [28] R.A. Fisher, A.S. Corbet, C. B. Williams, The relation between the number of species and the number of individuals in a random sample of animal population, *J. Anim. Ecol.* 12 (1943) 42–58. <https://doi.org/10.2307/1411>.
- [29] S. Franz, L. Peliti, Error threshold in simple landscapes, *J. Phys. A: Math. Gen.* 30 (1997) 4481–4487. <https://doi.org/10.1088/0305-4470/30/13/006>.
- [30] H. Fujisaka, *Statistical Mechanics of Nonequilibrium Systems*, Sangyo Tosho, Tokyo, 1998, in Japanese.
- [31] A. Fujiwara, S. Abe, E. Yamaha, F. Yamazaki, M.C. Yoshida, Uniparental chromosome elimination in the early embryogenesis of the inviable salmonid hybrids between mass salmon female and rainbow trout male, *Chromosoma* 106 (1997) 44–52.
- [32] D. Gaiotto, G.W. Moore, E. Witten, An introduction to the web-based formalism, arXiv:1506.04086v2 [hep-th] (2016). <https://arxiv.org/abs/1506.04086> (accessed 11 Mar 2019).

- [33] W.D. Hamilton, The genetical evolution of social behaviour, I, *J. Theor. Biol.* 7 (1964) 1–16. [https://doi.org/10.1016/0022-5193\(64\)90038-4](https://doi.org/10.1016/0022-5193(64)90038-4).
- [34] W.D. Hamilton, The genetical evolution of social behaviour, II, *J. Theor. Biol.* 7 (1964) 17–52. [https://doi.org/10.1016/0022-5193\(64\)90039-6](https://doi.org/10.1016/0022-5193(64)90039-6).
- [35] G.H. Hardy, J.E. Littlewood, Contributions to the theory of the Riemann zeta-function and the theory of the distribution of primes, *Acta Math.* 41 (1916) 119–196. <http://doi.org/10.1007/bf02422942>.
- [36] J. Harte, T. Zillio, E. Conlisk, A.B. Smith, Maximum entropy and the state-variable approach to macroecology, *Ecology* 89 (2008) 2700–2711. <https://doi.org/10.1890/07-1369.1>.
- [37] R. Hartshorne, *Algebraic Geometry*, Springer-Verlag, Berlin, New York, 1977.
- [38] S.P. Hubbell, A unified theory of biogeography and relative species abundance and its application to tropical rain forests and coral reefs, *Coral Reefs* 16 (1997) s9–s21. <https://doi.org/10.1007/s003380050237>.
- [39] S.P. Hubbell, *The Unified Neutral Theory of Biodiversity and Biogeography*, Princeton University Press, Princeton, 2001.
- [40] A. Juhl, *Cohomological Theory of Dynamical Zeta Functions*, Birkhäuser, Basel, 2001.
- [41] F. Károlyházy, Gravitation and quantum mechanics of macroscopic objects (*). *Il Nuovo Cimento* 52 (1966) 390–402. <https://doi.org/10.1007/BF02717926>.
- [42] F. Károlyházy, A. Frenkel, B. Lukács, On the possible role of gravity in the reduction of the wave function, in: R. Penrose, C. J. Isham, (Eds.), *Quantum Concepts in Space and Time*, Oxford University Press, Oxford, 1986, pp. 109–128.
- [43] N.M. Katz, *Twisted L-functions and Monodromy*, Princeton University Press, Princeton, 2009.

- [44] E.H. Kerner, A statistical mechanics of interacting biological species, *B. Math. Biol.* 19 (1957) 121–146. <https://doi.org/10.1007/BF02477883>.
- [45] M. Kimura, Diffusion models in population genetics, *J. Appl. Prob.* 1 (1964) 177–232. <https://doi.org/10.2307/3211856>.
- [46] M. Kisin, Moduli of finite flat group schemes, and modularity, *Ann. Math.* 170 (2009) 1085–1180. <https://doi.org/10.4007/annals.2009.170.1085>.
- [47] F. Klein, Neue Beiträge zur Riemannschen Funktionentheorie, *Math. Ann.* 21 (1883) 141–218. <https://doi.org/10.1007/BF01442920>.
- [48] F.C. Klein, Vorlesungen über das Ikosaeder und die Auflösung der Gleichungen vom fünften Grade, B.G. Teubner, Leipzig, 1993.
- [49] J. Knebel, M.F. Weber, T. Krüger, E. Frey, Evolutionary games of condensates in coupled birth-death processes, *Nat. Commun.* 6 (2015) 6977. <https://doi.org/10.1038/ncomms7977>.
- [50] D. Knuth, *The Art of Computer Programming, 2: Seminumerical Algorithms*, 3rd ed., Addison-Wesley Professional, Boston, 1997.
- [51] S. Kobayashi, K. Nomizu, *Foundations of Differential Geometry*, vol. 2, Wiley-Interscience, Hoboken, 1996.
- [52] P. Koebe, Über die Uniformisierung reeller analytischer Kurven, *Gött. Nachr.* 1907 (1907) 177–190.
- [53] P. Koebe, Über die Uniformisierung beliebiger analytischer Kurven, *Gött. Nachr.* 1907 (1907) 191–210.
- [54] P. Koebe, Über die Uniformisierung beliebiger analytischer Kurven (Zweite Mitteilung), *Gött. Nachr.* 1907 (1907) 633–669.
- [55] C.J. Krebs, *Ecology - The Experimental Analysis of Distribution and Abundance*, Harper International, New York, 1972.
- [56] N. Kurokawa, On certain Euler products, *Acta Arithmetica* 48 (1987) 49–52. <https://doi.org/10.4064/aa-48-1-49-52>.

- [57] M.L. Lapidus, G. Radunović, D. Žubrinić, *Fractal zeta functions and fractal drums*, Springer, Cham, 2017.
- [58] M.A. Leibold, M. Holyoak, N. Mouquet, P. Amarasekare, J.N. Chase, M.F. Hoopes, et al., The metacommunity concept: a framework for multi-scale community ecology, *Ecol. Lett.* 7 (2004) 601–613. <https://doi.org/10.1111/j.1461-0248.2004.00608.x>.
- [59] C. Lizama, J.G. Mesquita, Almost automorphic solutions of dynamic equations on time scales, *J. Funct. Anal.* 265 (2013) 2267–2311. <https://doi.org/10.1016/j.jfa.2013.06.013>.
- [60] A.J. Lotka, Natural selection as a physical principle, *Proc. Natl. Acad. Sci. USA* 8 (1922) 151–154. <https://doi.org/10.1073/pnas.8.6.151>.
- [61] M. Marinō, Lectures on non-perturbative effects in large \mathcal{N} gauge theories, matrix models and strings, *Fortschr. Phys.* 62 (2014) 455–540. <https://doi.org/10.1002/prop.201400005>.
- [62] G. Marinoni, M. Manuel, R.F. Petersen, J. Hvidtfeldt, P. Sulo, J. Piskur, Horizontal transfer of genetic material among *Saccharomyces* yeasts, *J. Bacteriol.* 181 (1999) 6488–6496.
- [63] E. Mayr, *Systematics and the Origin of Species*, Columbia University Press, New York, 1942.
- [64] L. Medlin, H.J. Elwood, S. Stickel, M.L. Sogin, The characterization of enzymatically amplified eukaryotic 16S-like rRNA-coding regions, *Gene* 71 (1988) 491–499. [https://doi.org/10.1016/0378-1119\(88\)90066-2](https://doi.org/10.1016/0378-1119(88)90066-2).
- [65] G.J. Mendel, Versuche über Pflanzenhybriden, *Verhandlungen des naturforschenden Vereines in Brünn*, Bd IV für das Jahr, 1865, Abhandlungen (1866) 3–47. <https://doi.org/10.5962/bhl.title.61004>.
- [66] J. Milnor, *Morse Theory*, Princeton University Press, Princeton, 1969.
- [67] R.L. Mkrtychyan, A.P. Veselov, Universality in Chern-Simons theory, *J. High Energy Phys.* 2012 (2012) 153. [https://doi.org/10.1007/JHEP08\(2012\)153](https://doi.org/10.1007/JHEP08(2012)153).
- [68] Y. Motohashi, *Spectral Theory of the Riemann Zeta-Function*, Cambridge University Press, Cambridge, 1997.

- [69] S. Mukai, Finite groups of automorphisms of K3 surfaces and the Mathieu group, *Invent. Math.* 94 (1988) 183–221. <https://doi.org/10.1007/BF01394352>.
- [70] J. Neukirch, *Algebraic Number Theory*, Springer-Verlag, Berlin-Heidelberg-New York, 1999.
- [71] S. Odake, R. Sasaki, Reflectionless potentials for difference Schrödinger equations, *J. Phys. A: Math. Theor.* 48 (2015) 115204. <https://doi.org/10.1088/1751-8113/48/11/115204>.
- [72] S.J. Phillips, R.P. Anderson, R.E. Schapire, Maximum entropy modeling of species geographic distributions, *Ecol. Model.* 190 (2006) 231–259. <https://doi.org/10.1016/j.ecolmodel.2005.03.026>.
- [73] S. Pigolotti, A. Flammini, M. Marsili, A. Maritan, Species lifetime distribution for simple models of ecologies, *Proc. Natl. Acad. Sci. USA* 102 (2005) 15747–15751. <https://doi.org/10.1073/pnas.0502648102>.
- [74] H. Poincaré, Mémoire sur les fonctions fuchsiennes, *Acta Math.* 1 (1882) 193–294. <https://doi.org/10.1007/BF02592135>.
- [75] H. Poincaré, Sur un théorème de la théorie générale des fonctions, *Bull. Soc. Math. Fr.* 11 (1883) 112–125. <https://doi.org/10.24033/bsmf.261>.
- [76] H. Poincaré, Sur l’uniformisation des fonctions analytiques, *Acta Math.* 3 (1907) 1–63. <https://doi.org/10.1007/BF0241544>. <https://doi.org/10.1007/BF0241544>.
- [77] G.R. Price, Selection and covariance, *Nature* 227 (1970) 520–521. <https://doi.org/10.1038/227520a0>.
- [78] S. Pueyo, F. He, T. Zillio, The maximum entropy formalism and the idiosyncratic theory of biodiversity, *Ecol. Lett.* 10 (2007) 1017–1028. <https://doi.org/10.1111/j.1461-0248.2007.01096.x>.
- [79] A.P. Rasnitsyn, The problem of species revisited, *Paleontol. J.* 41 (2007) 1151–1155. <https://doi.org/10.1134/S0031030107110135>.
- [80] J. Ray, *Historia Plantarum*, vol. 1, T. Primus, London, 1686.

- [81] B. Riemann, Ueber die Anzahl der Primzahlen unter einer gegebenen Größe, Monatsber. Berl. Akad. 1859 (1859) 671–680.
- [82] R.A. Rodr—íguez, J.D. Delgado, A.M. Herrera, R. Riera, R.M. Navarro, C. Melia'n, et al., Effects of two traits of the ecological state equation on our understanding of species coexistence and ecosystem services, *Ecol. Model.* 265 (2013) 1–13. <https://doi.org/10.1016/j.ecolmodel.2013.06.001>.
- [83] R.A. Rodr—íguez, A.M. Herrera, J.D. Delgado, R. Otto, Á. Quirós, J. Santander, et al., Biomass-dispersal trade-off and the functional meaning of species diversity, *Ecol. Model.* 261/262 (2013) 8–18. <https://doi.org/10.1016/j.ecolmodel.2013.03.023>.
- [84] R.A. Rodr—íguez, A.M. Herrera, R. Riera, C.G. Escudero, J.D. Delgado, Empirical clues about the fulfillment of quantum principles in ecology: potential meaning and theoretical challenges, *Ecol. Model.* 301 (2015) 90–97. <https://doi.org/10.1016/j.ecolmodel.2015.01.023>.
- [85] C. Sabbah, Théorie de Hodge et théorème de Lefschetz « difficile », in: C. Sabbah, Notes de Cours 2000/2001, 2001. <http://www.math.polytechnique.fr/cmat/sabbah/livres/hodge-str.pdf> (accessed 11 Mar 2019).
- [86] C.E. Shannon, A mathematical theory of communication, *Bell Syst. Tech. J.* 27 (1948) 379–423/623–656. <https://doi.org/10.1002/j.1538-7305.1948.tb01338.x>. <https://doi.org/10.1002/j.1538-7305.1948.tb00917.x>.
- [87] H. Shimodaira, Testing regions with nonsmooth boundaries via multiscale bootstrap, *J. Stat. Plan. Inference* 138 (2008) 1227–1241. <https://doi.org/10.1016/j.jspi.2007.04.001>.
- [88] H. Shimodaira, T. Kanamori, M. Aoki, K. Mine, Multiscale bagging and its applications, *IEICE Trans. Inf. & Syst.* E94-D (2011) 1924–1932. <https://doi.org/10.1587/transinf.E94.D.1924>.
- [89] J.M. Smith, Group selection and kin selection. *Nature* 201 (1964) 1145–1147. <https://doi.org/10.1038/2011145a0>.

- [90] E. Sober, D.S. Wilson, *Unto Others: The Evolution and Psychology of Unselfish Behavior*, Harvard University Press, Cambridge, 1998.
- [91] B. Spagnolo, D. Valenti, A. Fiasconaro, Noise in ecosystems: a short review, *Math. Biosci. Eng.* 1 (2004) 185–211. <https://doi.org/10.3934/mbe.2004.1.185>.
- [92] P.J. Steinhardt, N. Turok, The cyclic model simplified. *New Astron. Rev.* 49 (2004) 43–57. <https://doi.org/10.1016/j.newar.2005.01.003>.
- [93] M.H. Stone, Linear transformations in Hilbert space: III, Operational methods and group theory, *Proc. Natl. Acad. Sci. USA* 16 (1930) 172–175. <https://doi.org/10.1073/pnas.16.2.172> .
- [94] M.H. Stone, On one-parameter unitary groups in Hilbert space, *Ann. Math.* 33 (1932) 643–648. <https://doi.org/10.2307/1968538>.
- [95] L. Sylow, Théorèmes sur les groupes de substitutions, *Math. Ann.* 5 (1872) 584–594. <https://doi.org/10.1007/BF01442913>.
- [96] Y. Tachikawa, K. Yonekura, Gauge interactions and topological phase of matter, *Prog. Theor. Exp. Phys.* 2016 (2016) 093B07. <https://doi.org/10.1093/ptep/ptw131>.
- [97] H. Tasaki, T. Hara, *Mathematical Principles of Phase Transitions and Critical Phenomena*, Kyoritsu Shuppan, Tokyo, 2015, in Japanese.
- [98] R. Taylor, A. Wiles, Ring-theoretic properties of certain Hecke algebras, *Ann. Math.* 141 (1995) 553–572. <https://doi.org/10.2307/2118560>.
- [99] Y. Terashima, M. Yamazaki, Semiclassical analysis of the 3d/3d Relation, *Phys. Rev. D* 88 (2013) 026011. <https://doi.org/10.1103/PhysRevD.88.026011>.
- [100] M. Tribus, Information theory as the basis for thermostatics and thermodynamics, *J. Appl. Mech.* 28 (1961) 1–8. <https://doi.org/10.1115/1.3640461>.
- [101] R.L. Trivers, The evolution of reciprocal altruism, *Q. Rev. Biol.* 46 (1971) 35–57. <https://doi.org/10.1086/406755>.

- [102] I. Volkov, J.R. Banavar, Organization of ecosystems in the vicinity of a novel phase transition, *Phys. Rev. Lett.* 92 (2004) 218703. <https://doi.org/10.1103/PhysRevLett.92.218703>.
- [103] C. von Linné, *Systema Naturæ*, T. Haak, Leiden, 1735.
- [104] H. von Mangoldt, Zur Verteilung der Nullstellen der Riemannschen Funktion $\gamma(t)$, *Math. Ann.* 60 (1905) 1–19. <https://doi.org/10.1007/BF01447494>.
- [105] J. von Neumann, Die Eindeutigkeit der Schrödingerschen Operatoren, *Math. Ann.* 104 (1931) 570–578. <https://doi.org/10.1007/BF01457956>.
- [106] J. von Neumann, Ueber Einen Satz von Herrn M. H. Stone, *Ann. Math. Ser. 2* 33 (1932) 567–573. <https://doi.org/10.2307/1968535>.
- [107] A.R. Wallace, On the tendency of varieties to depart indefinitely from the original type, *Zool. J. Linn. Soc.* 3 (1858) 53–62. <https://doi.org/10.1017/CBO9780511693106.004>.
- [108] S. Watanabe, Asymptotic equivalence of Bayes cross validation and Widely Applicable Information Criterion in singular learning theory, *J. Mach. Learn Res.* 11 (2010) 3571–3594.
- [109] A. Weil, Sur les “formules explicites” de la théorie des nombres premiers, *Comm. Sémin. Math. Univ. Lund [Medd. Lunds Univ. Mat. Sem.] Suppl.-band M. Riesz 1952 (1952) 252–265*. <https://doi.org/10.1070/IM1972v006n01ABEH001866>.
- [110] H. Weyl, *Die Idee der Riemannschen Fläche*, B.G. Teubner, Stuttgart, 1913.
- [111] C.R. White, R.S. Seymour, Mammalian basal metabolic rate is proportional to body mass^{2/3}, *Proc. Natl. Acad. Sci. USA* 100 (2003) 4046–4049. <https://doi.org/10.1073/pnas.0436428100>.
- [112] T.G. Whitham, J.K. Bailey, J.A. Schweitzer, S.M. Shuster, R.K. Bangert, C.J. LeRoy, et al., A framework for community and ecosystem genetics: from genes to ecosystems, *Nat. Rev. Genet.* 7 (2006) 510–523. <https://doi.org/10.1038/nrg1877>.

- [113] A. Wiles, Modular elliptic curves and Fermat's last theorem, *Ann. Math.* 142 (1995) 443–551. <https://doi.org/10.2307/2118559>.
- [114] D.S. Wilson, E. Sober, Reintroducing group selection to the human behavioral sciences, *Behav. Brain Sci.* 17 (1994) 585–654. <https://doi.org/10.1017/S0140525X00036104>.
- [115] E. Witten, Quantum field theory and the Jones polynomial, *Commun. Math. Phys.* 121 (1989) 351–399. <https://doi.org/10.1007/BF01217730>.
- [116] E. Witten, The “parity” anomaly on an unorientable manifold, *Phys. Rev. B* 94 (2016) 195150. <https://doi.org/10.1103/PhysRevB.94.195150>.
- [117] D. Zagier, Aspects of complex multiplication, in: *Notes of the Seminar Written by J. Voight*, 2000. <https://math.dartmouth.edu/~jvoight/notes/274-Zagier.pdf> (accessed 11 Mar 2019).
- [118] D. Zagier, Traces of singular moduli, in: *SIS-2004-265*, 2000. <http://cds.cern.ch/record/738436/files/sis-2004-265.ps> (accessed 11 Mar 2019).